

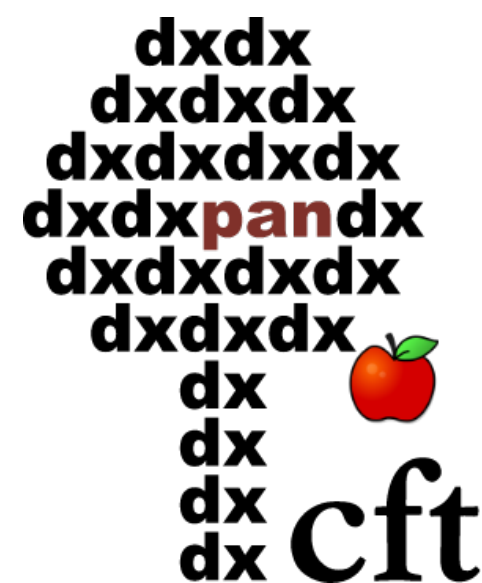
Numerical simulations of Long Gamma Ray Bursts from small to large scales

Gerardo Urrutia

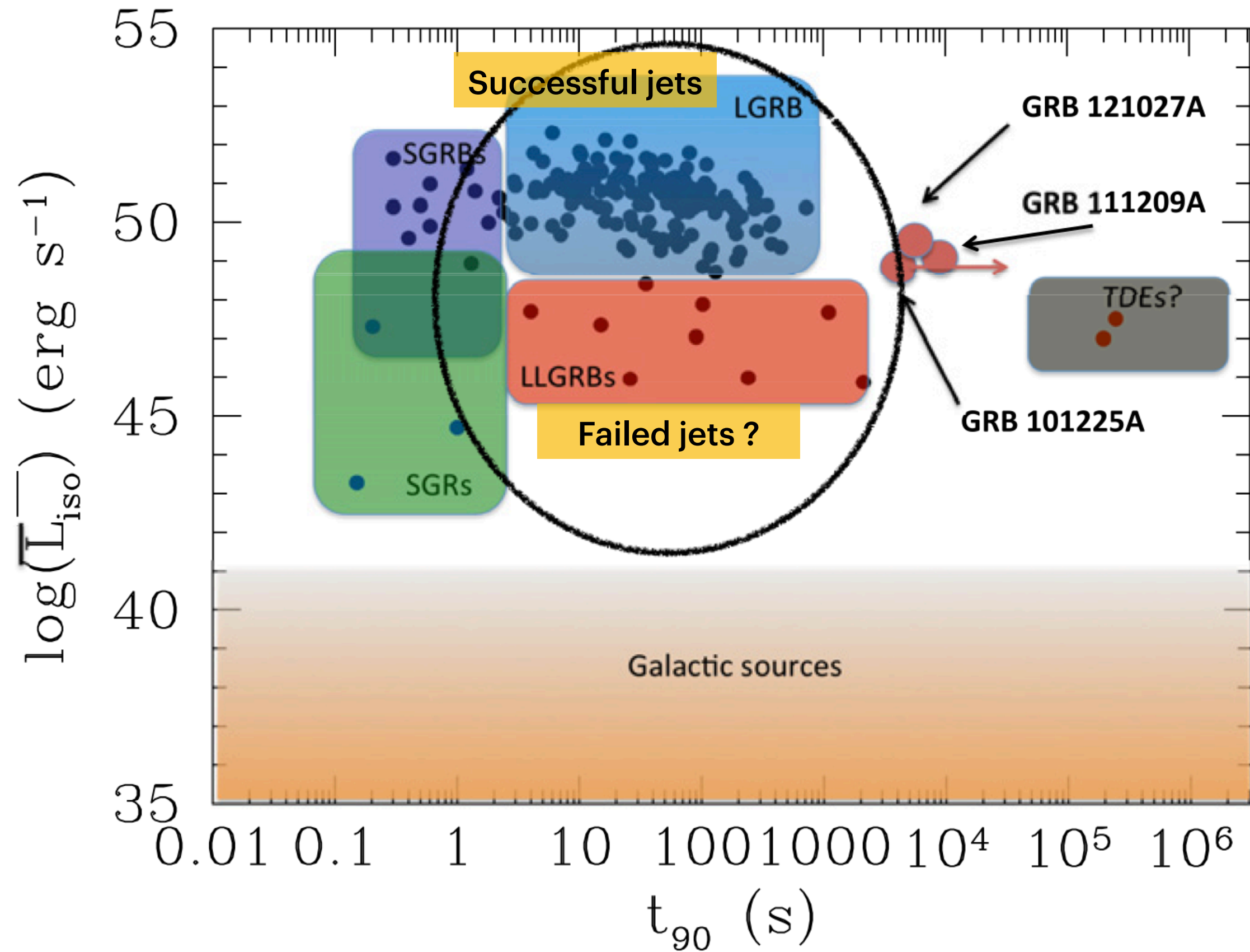
Center for Theoretical Physics, Warsaw, Poland

gurrutia@cft.edu.pl

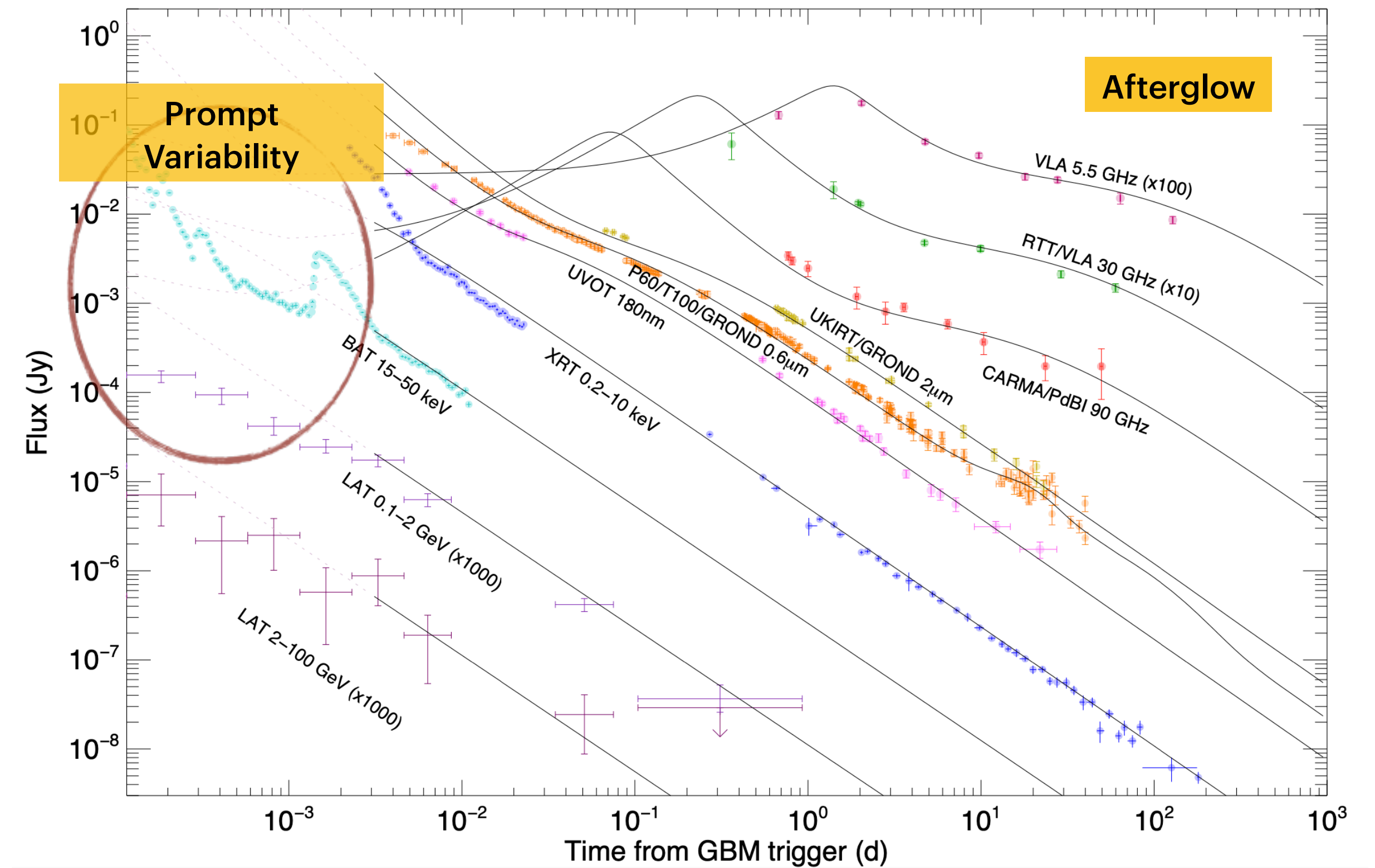
Agnieszka Janiuk (CFT, Poland), Hector Olivares (UA, Portugal)



Long GRBs



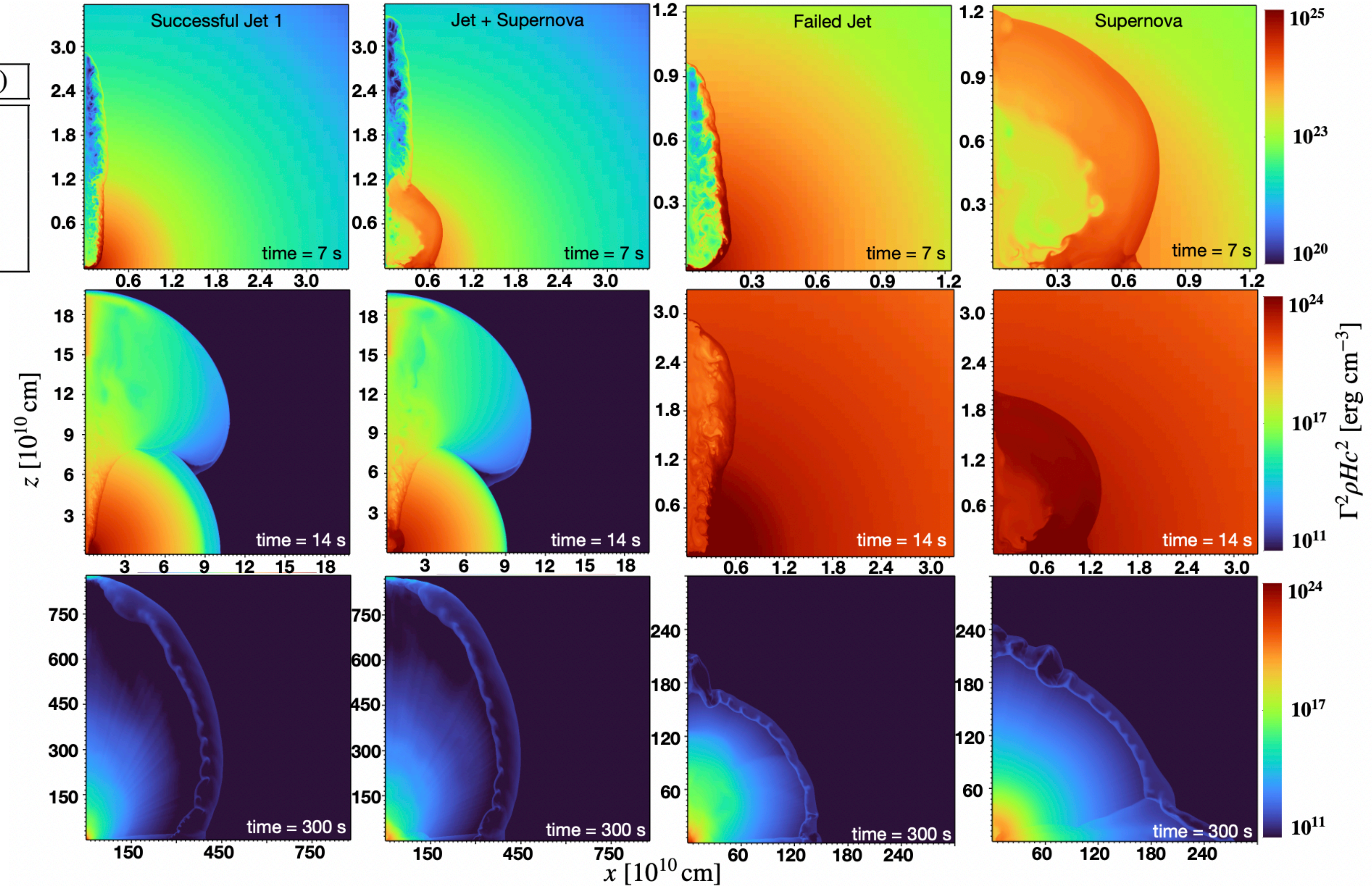
Levan et al. 2014



GRB 130427, Perley et al. 2013

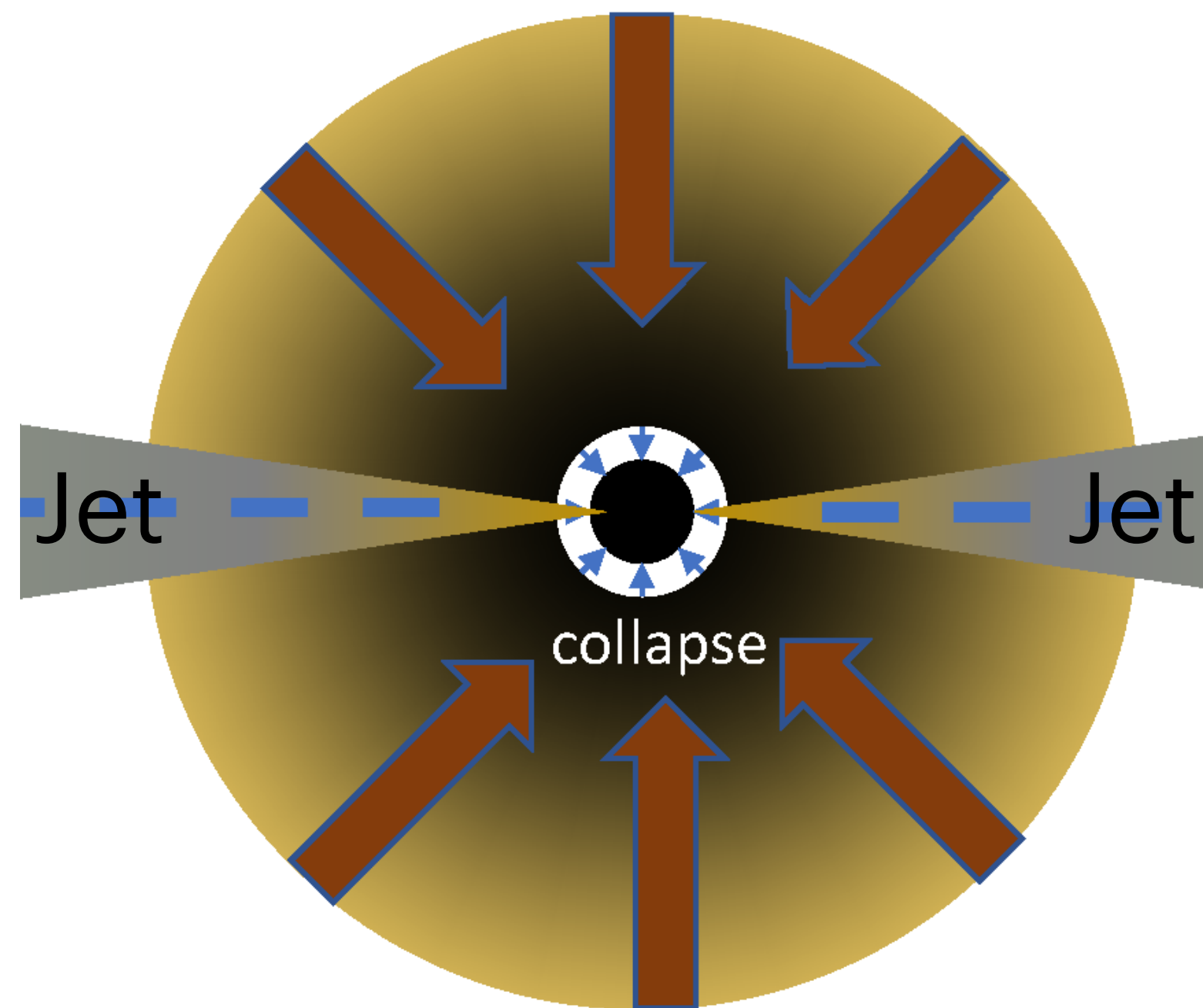
Jet dynamics

Scenario	t_{inj} (s)	Energy (erg)
Successful jet	10	10^{51}
Successful jet	2.5	10^{52}
Failed jet	10	10^{51}
Supernova	1	10^{52}
Jet + Supernova	10	10^{51}



Urrutia et al. 2023

The collapse of massive star produce a Long GRB



- Fast spinning BH (MacFadyen & Woosley 1999)
- Angular momentum distribution
- Funnel

$$t_{\text{dyn}} \sim 10\text{s}$$

$$\dot{M} \sim 0.1M_{\odot}\text{s}^{-1}$$

- Magneto rotational core collapse (Mösta 2014; 2015; Obergaulinger & Aloy 2020; Gottlieb 2022)

$$B_0 \sim 10^{14} - 10^{15}\text{G}$$

Long GRB Jet is a multi-scale problem

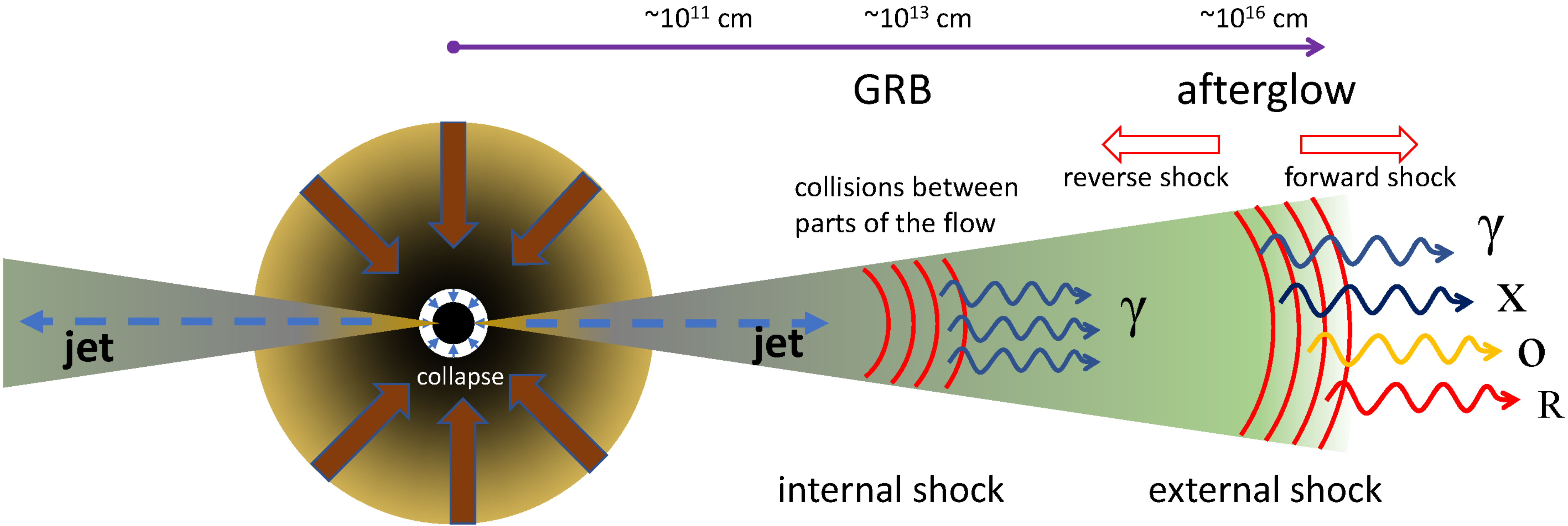
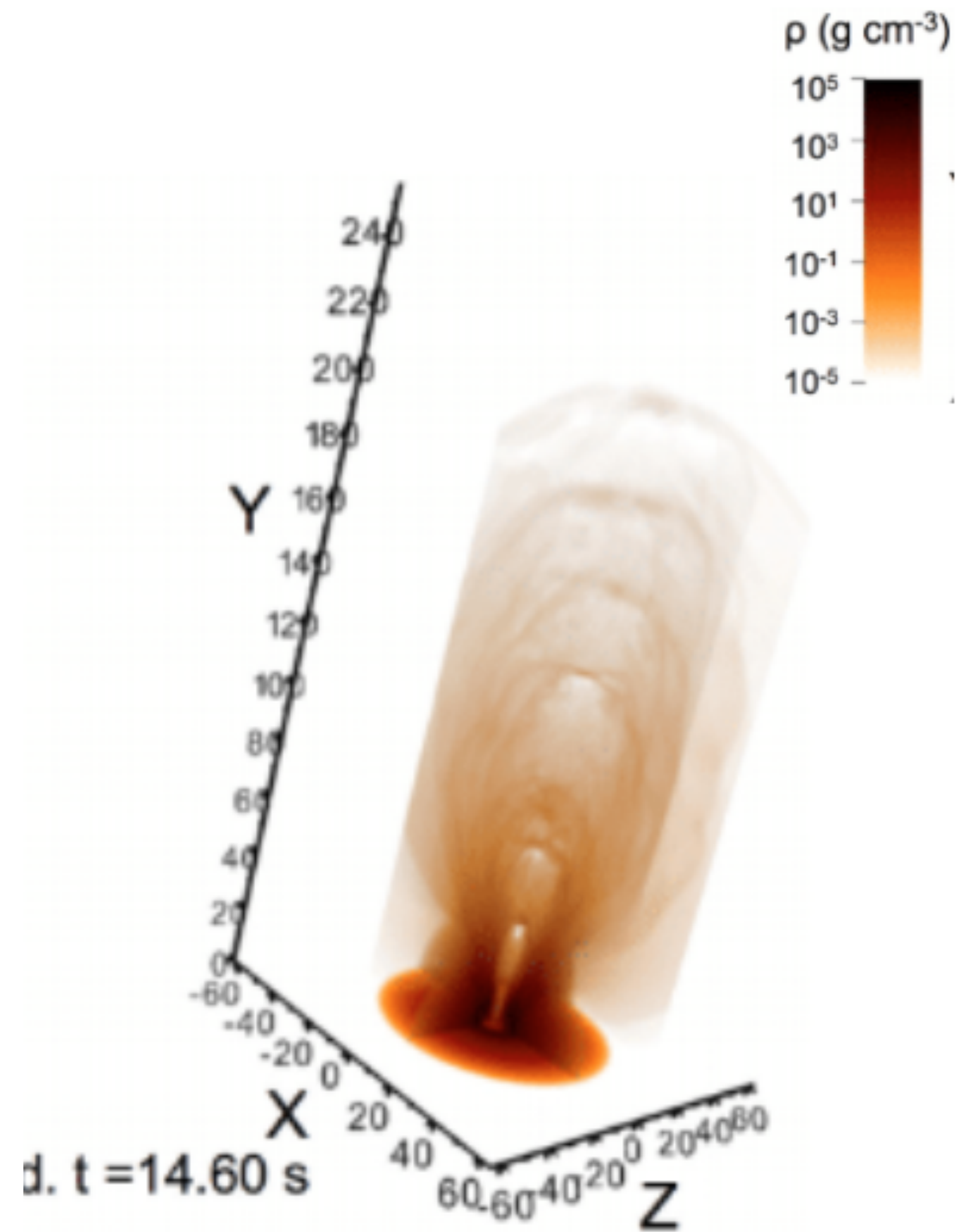


Figure Credits: Dado et al. 2022

Launching point far from the central engine

Launching point far from the central engine

Non symmetric (variable source)

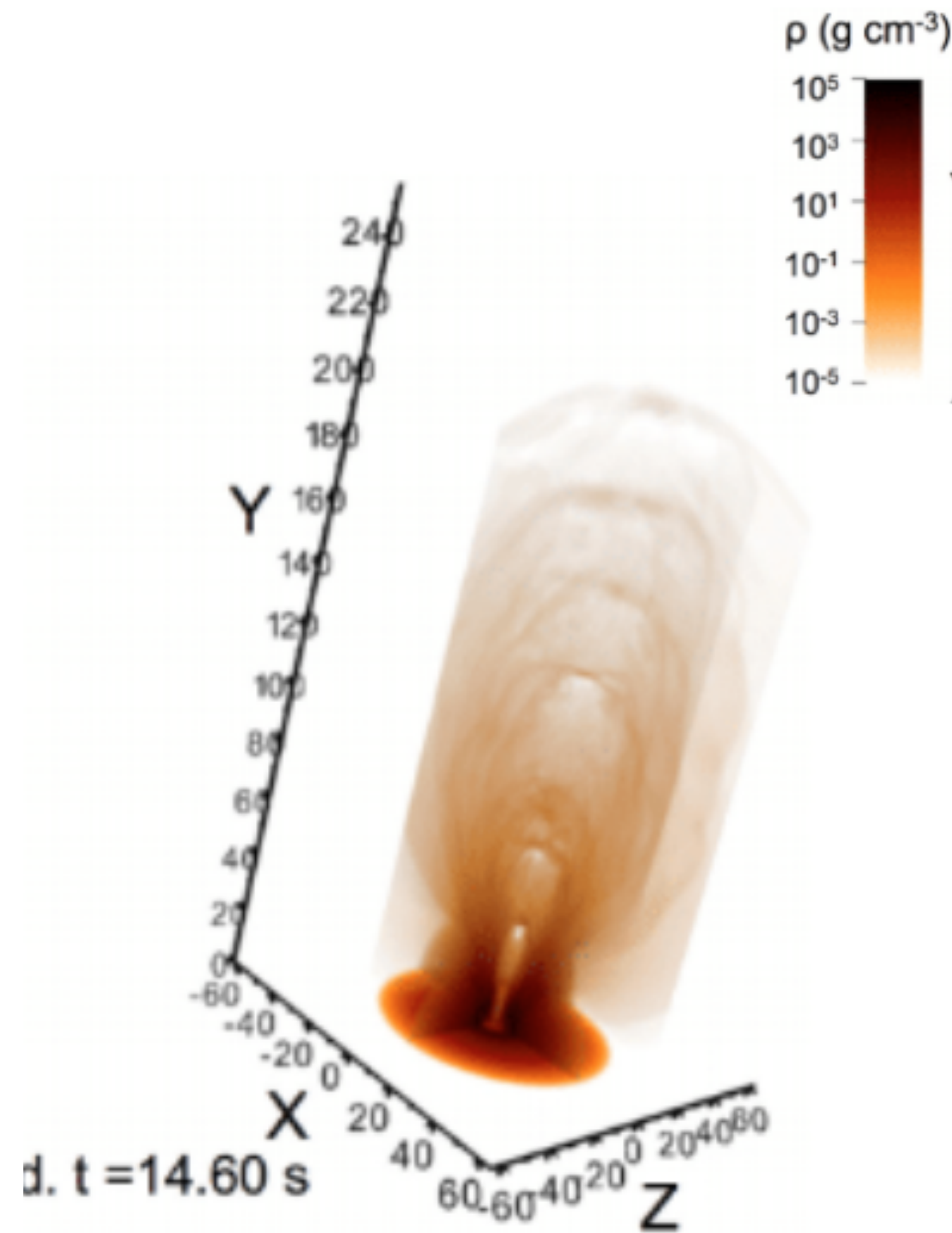


Lopez-Camara et al. 2016

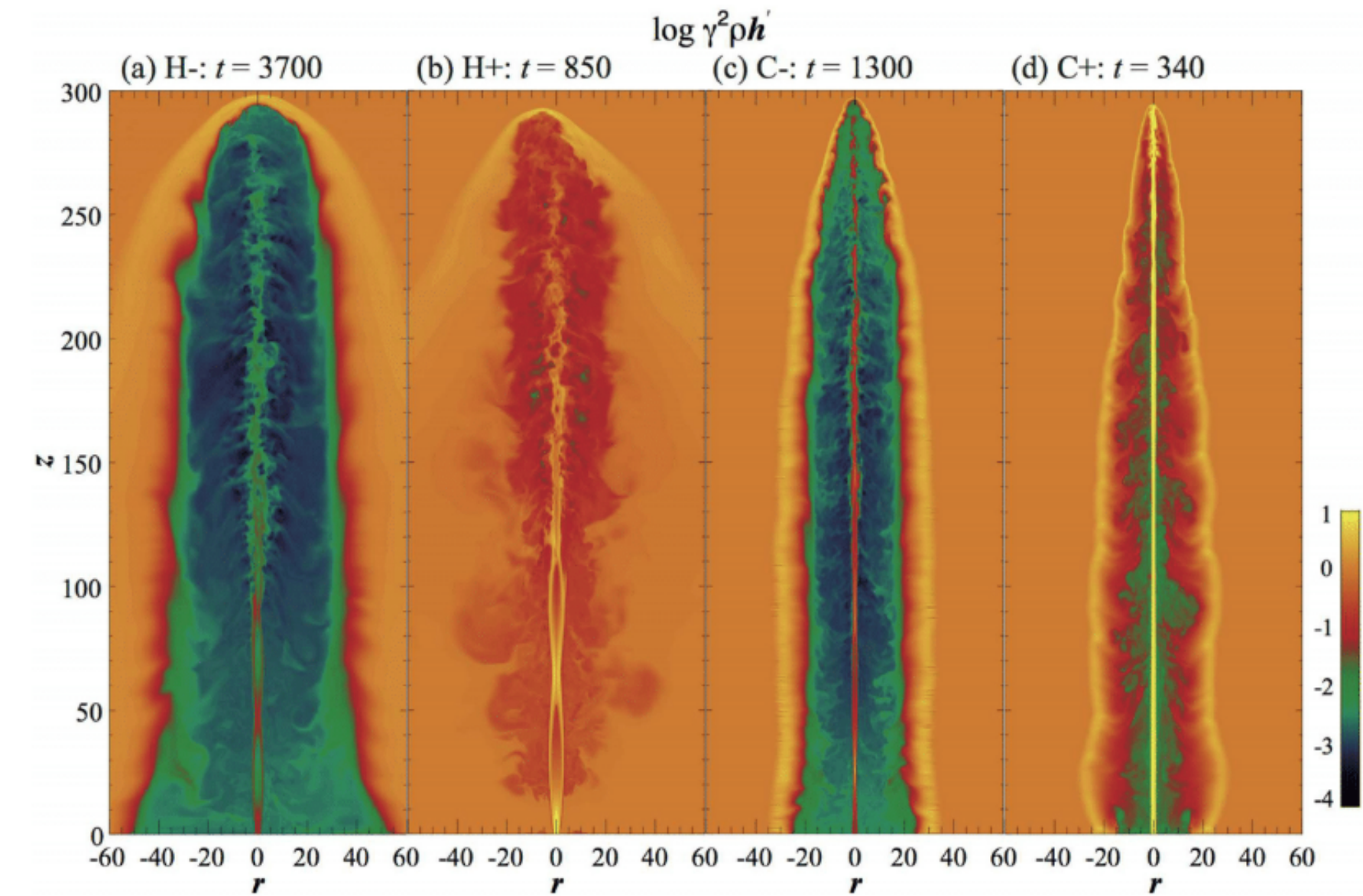
Launching point far from the central engine

Kinetic or pressure dominated jets

Non symmetric (variable source)



Lopez-Camara et al. 2016

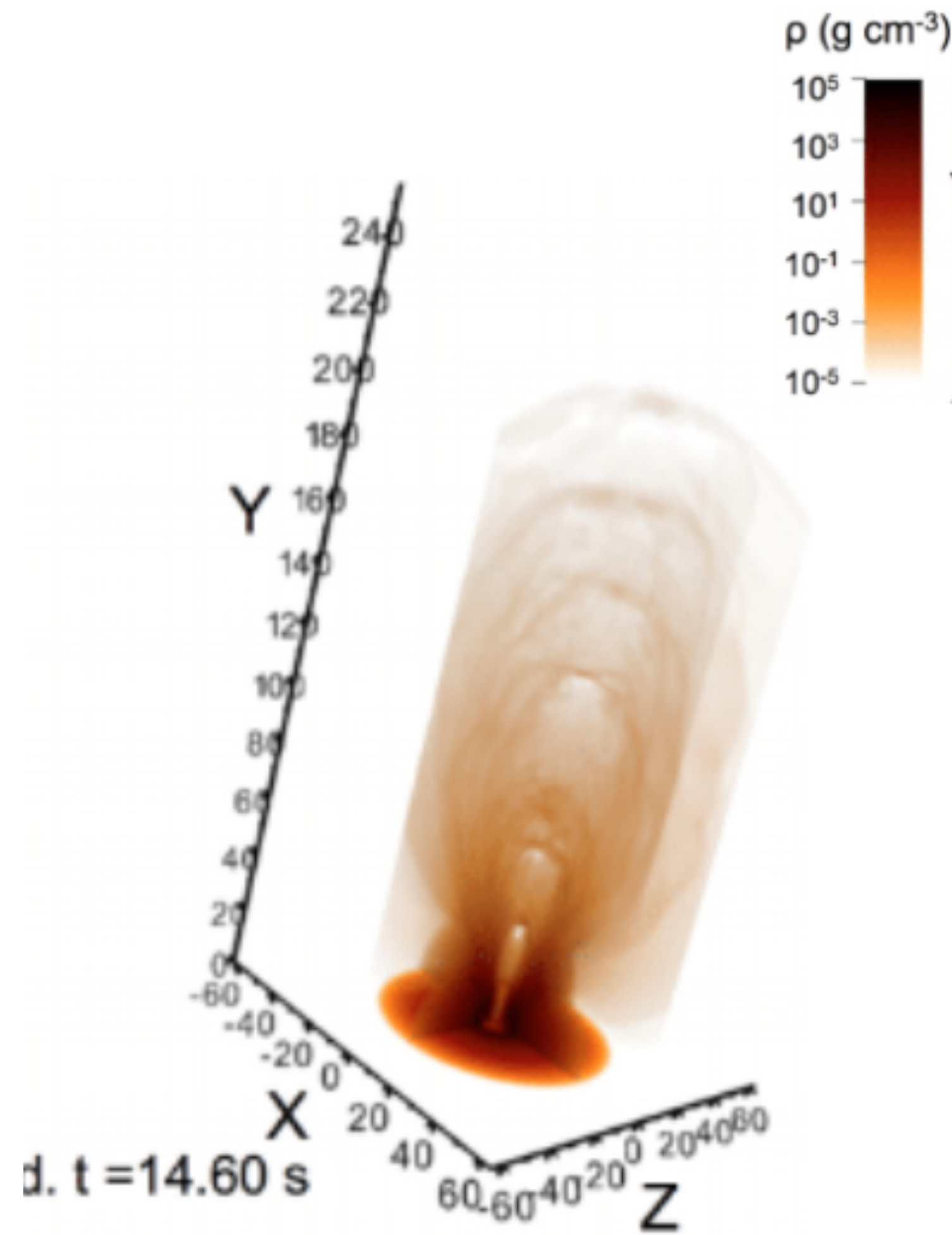


Matsumoto et al. 2019

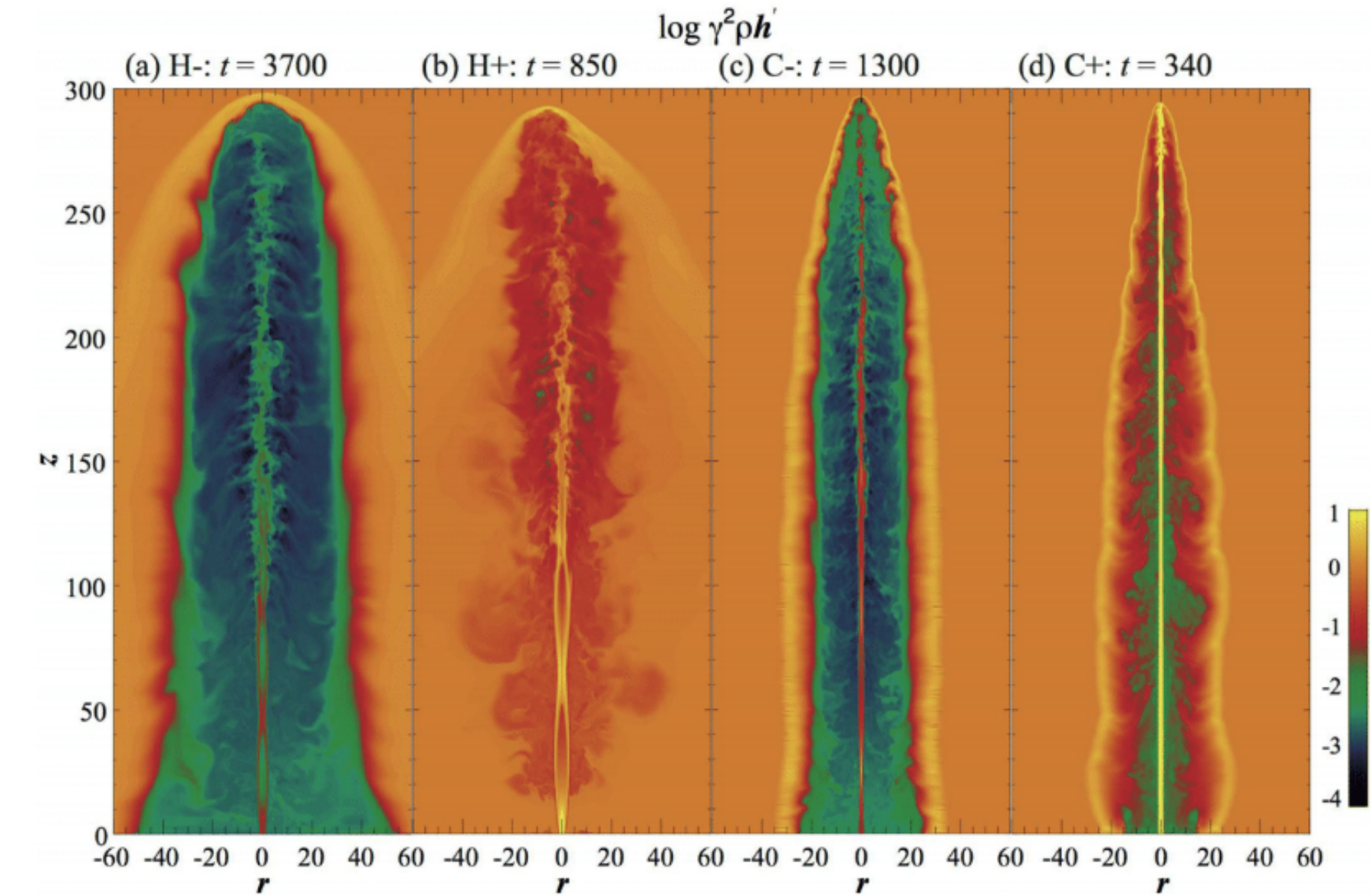
Launching point far from the central engine

Kinetic or pressure dominated jets

Non symmetric (variable source)

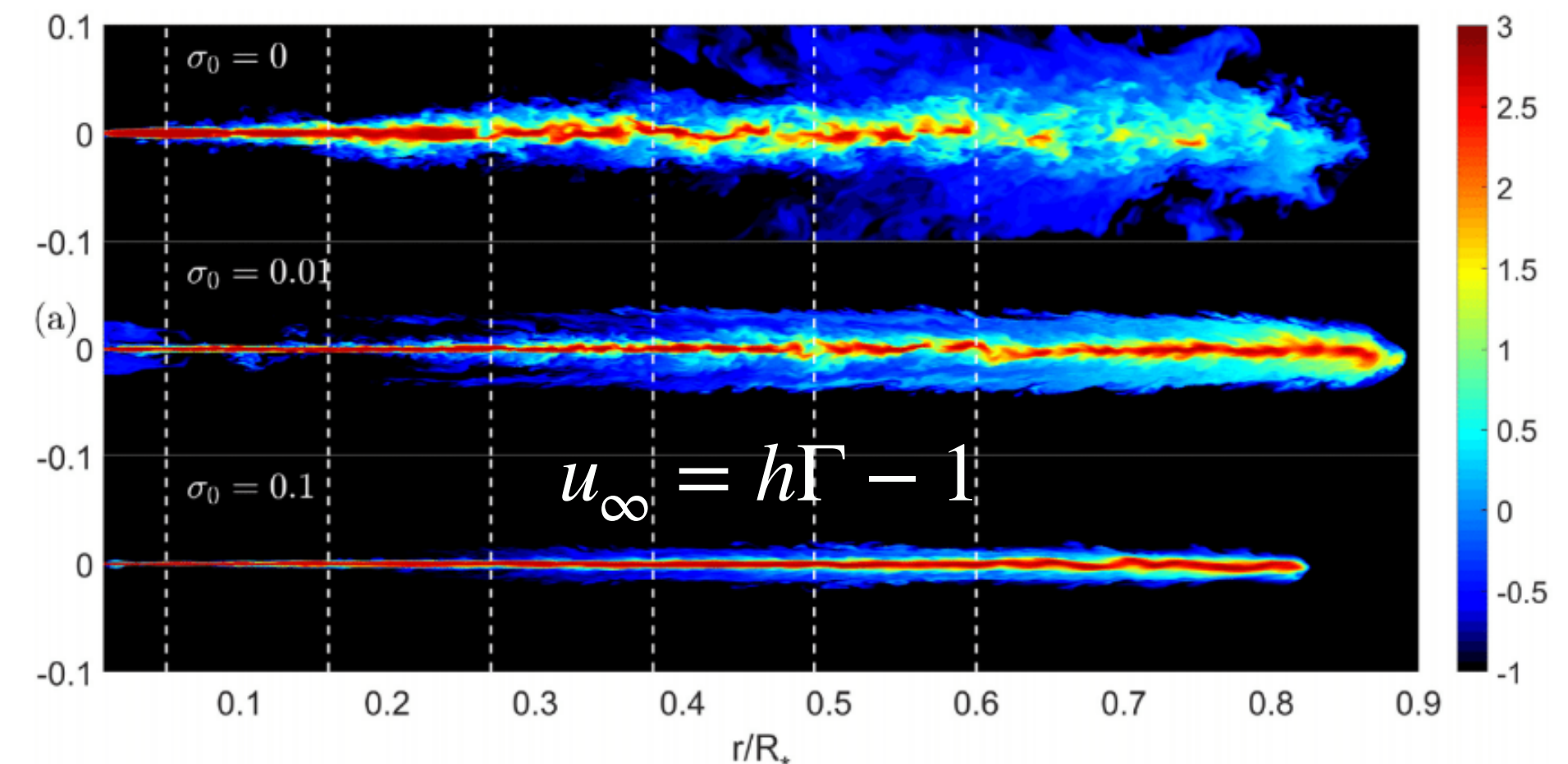


Lopez-Camara et al. 2016



Matsumoto et al. 2019

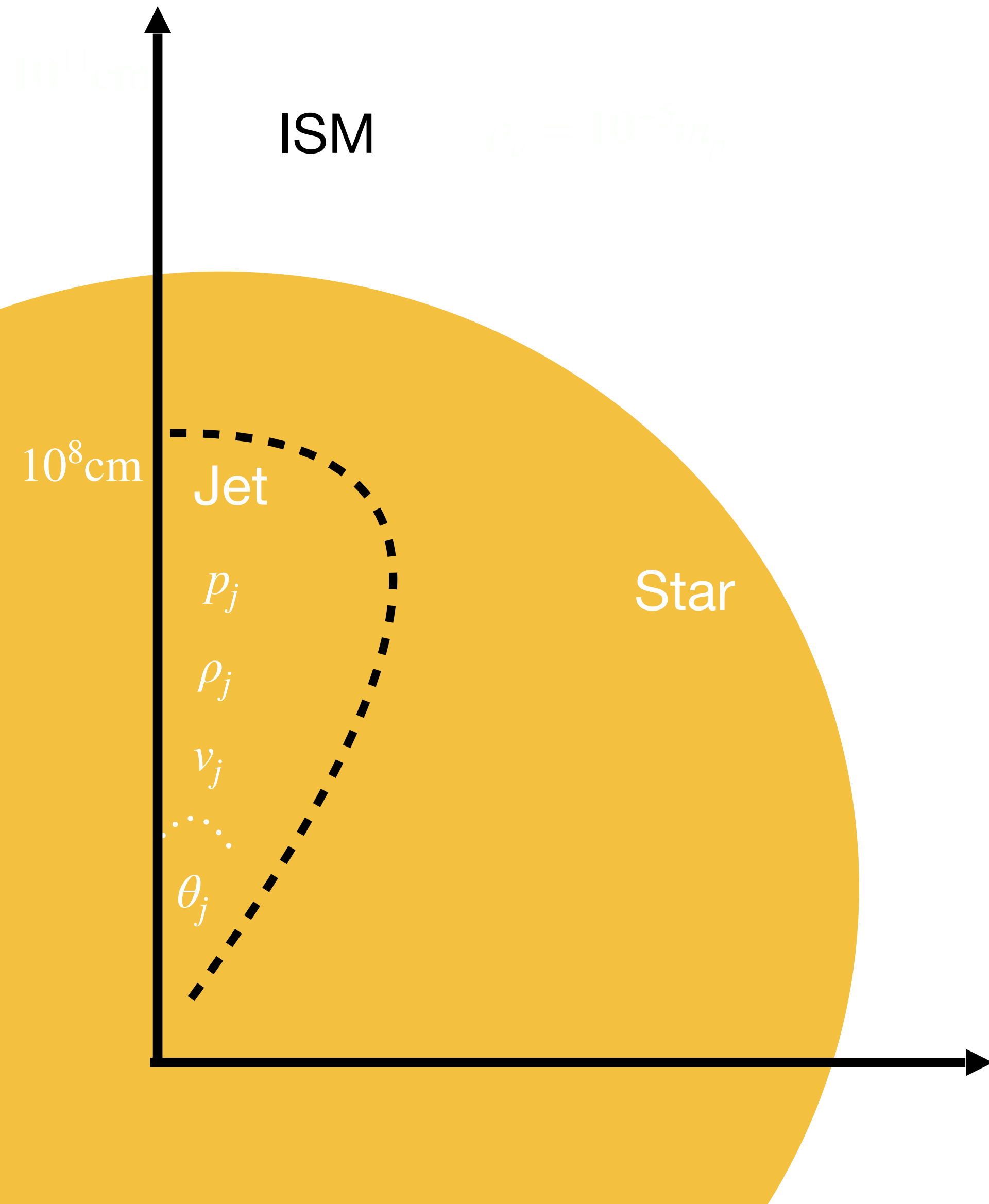
Weakly magnetized jet + variable source



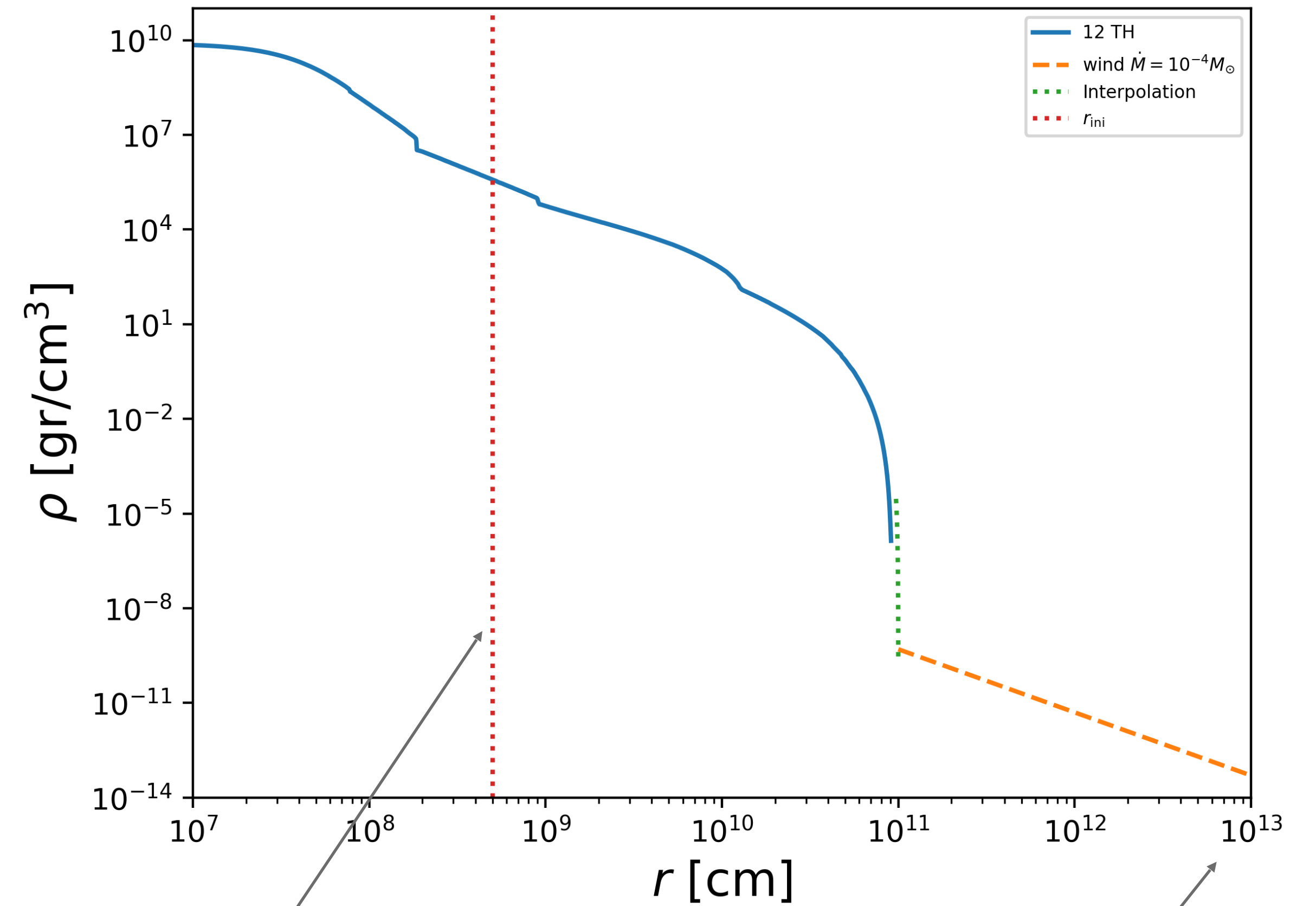
Gottlieb et al. 2020

Intermediate scales

The jet is imposed as a strong shock condition



- Stellar striped envelope WR (Woosley & Heger 2006)

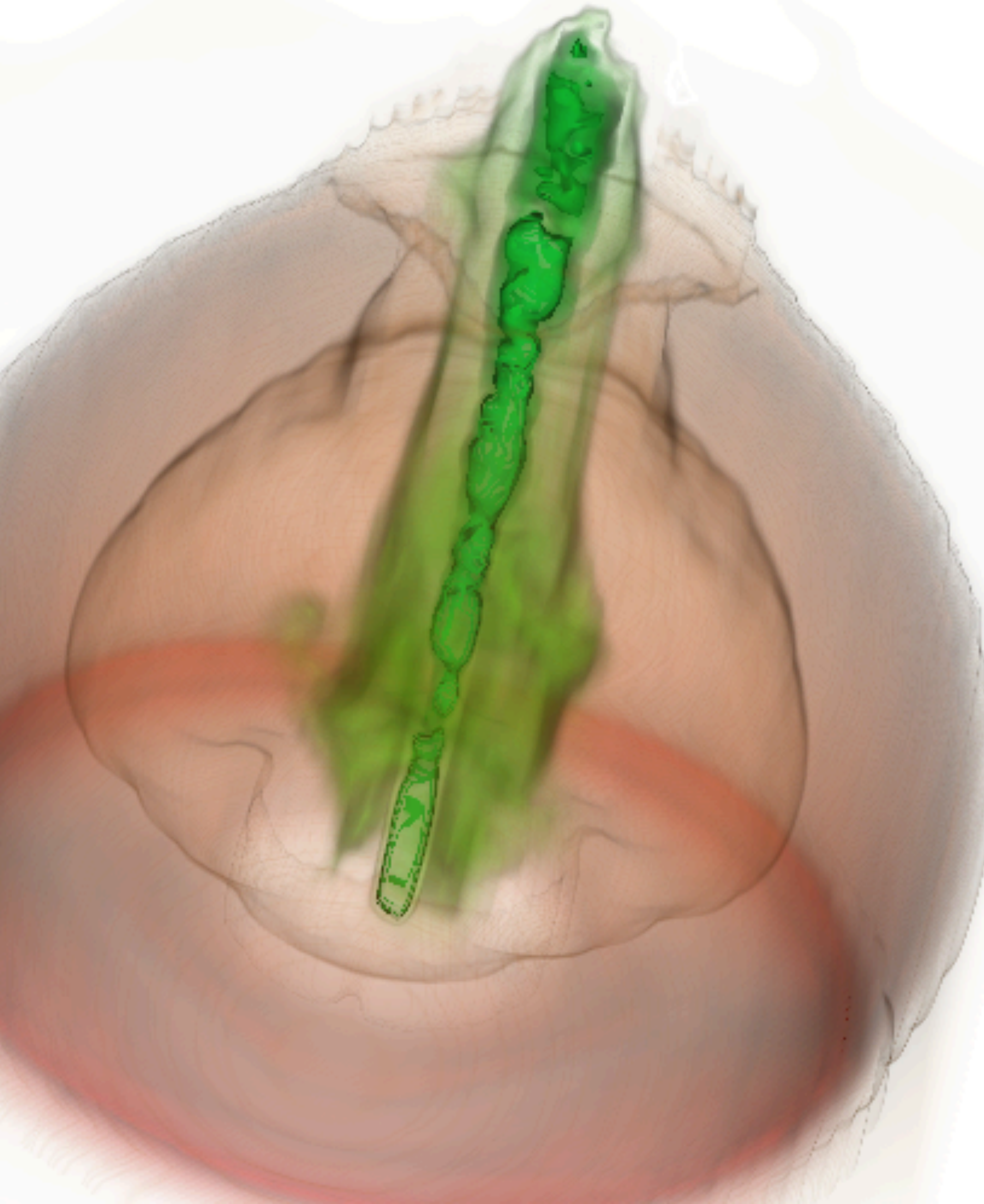


Initial Conditions

Size of AMR computational box

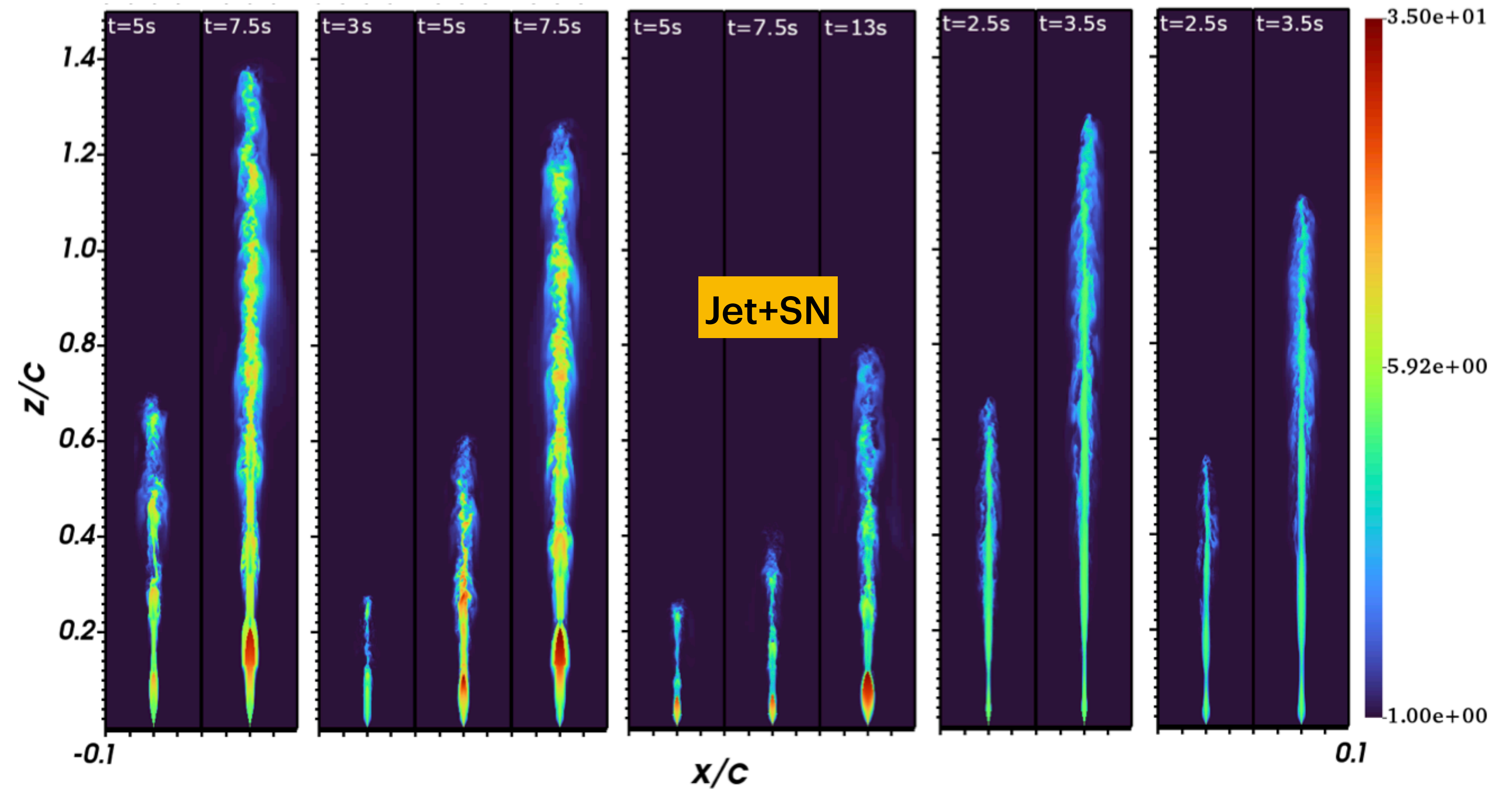
Jets initially structured

Gaussian jet + Supernova



Pressure dominated

Kinetic Dominated

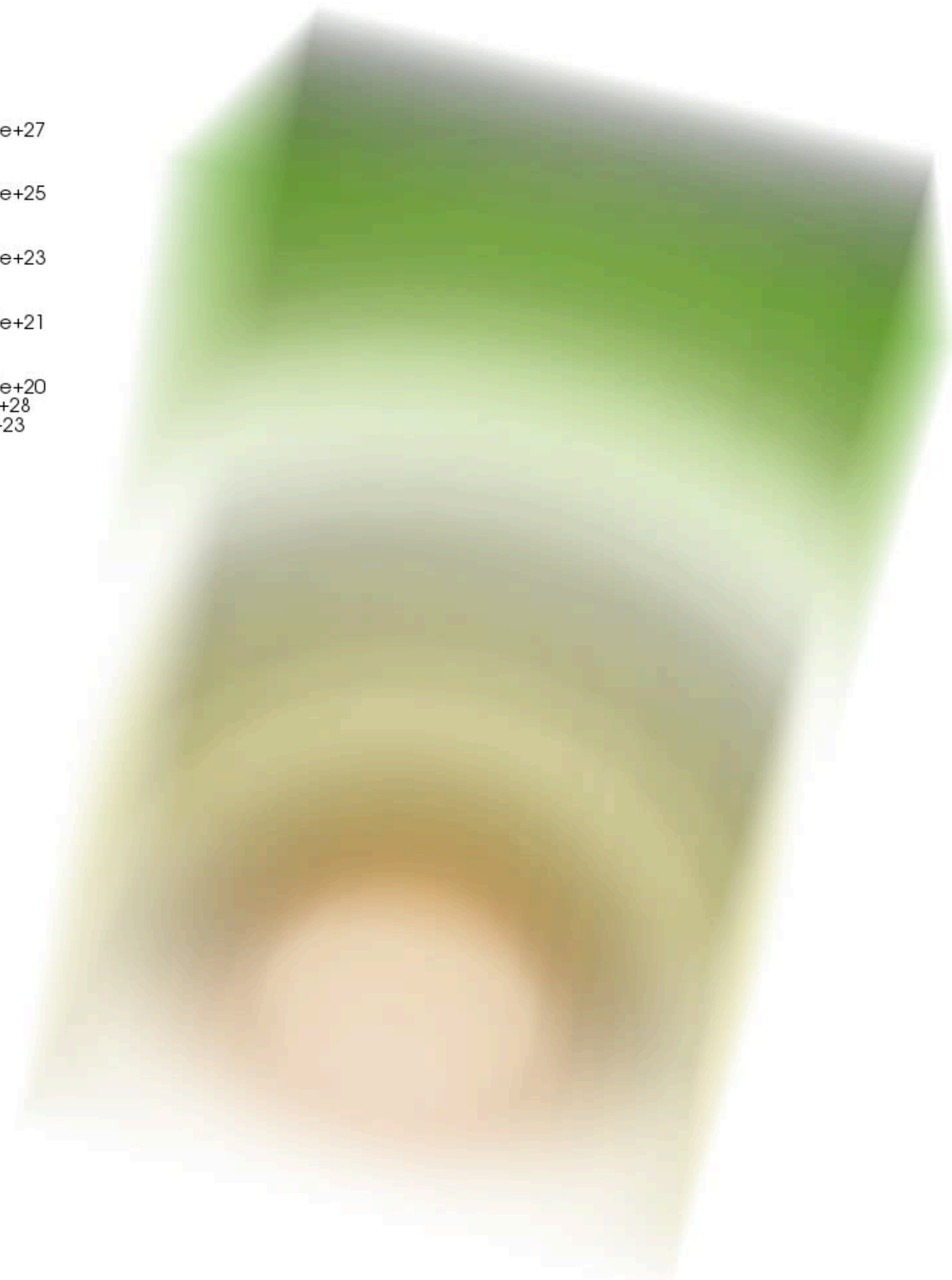


Urrutia, De Colle & Lopez-Camara 2023

Jets initially structured

Gaussian jet + Supernova

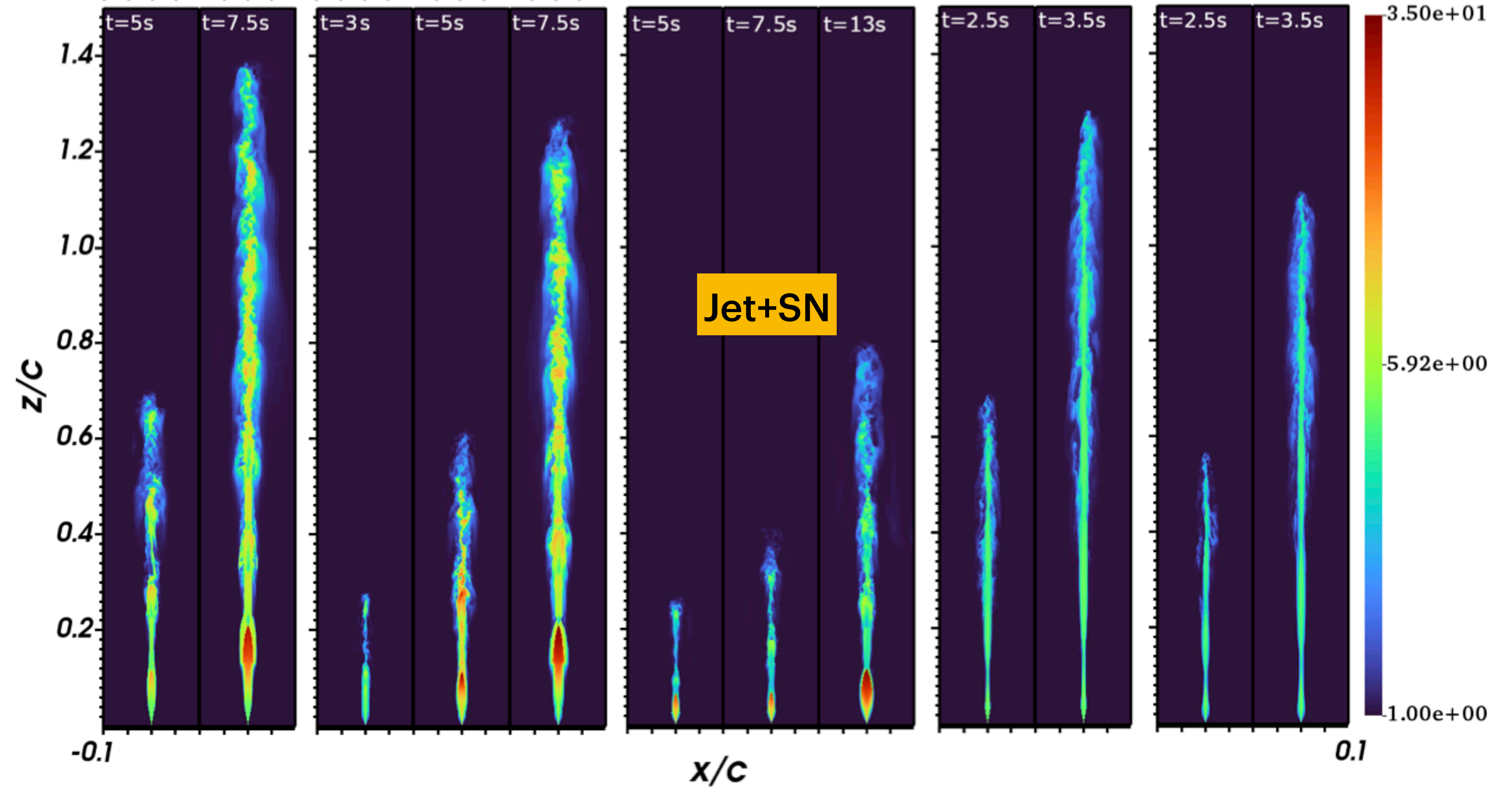
Volume
Var: de
2.000e+27
2.991e+25
4.472e+23
6.687e+21
1.000e+20
Max: 3.718e+28
Min: 4.239e+23



Time=0

Pressure dominated

Kinetic Dominated

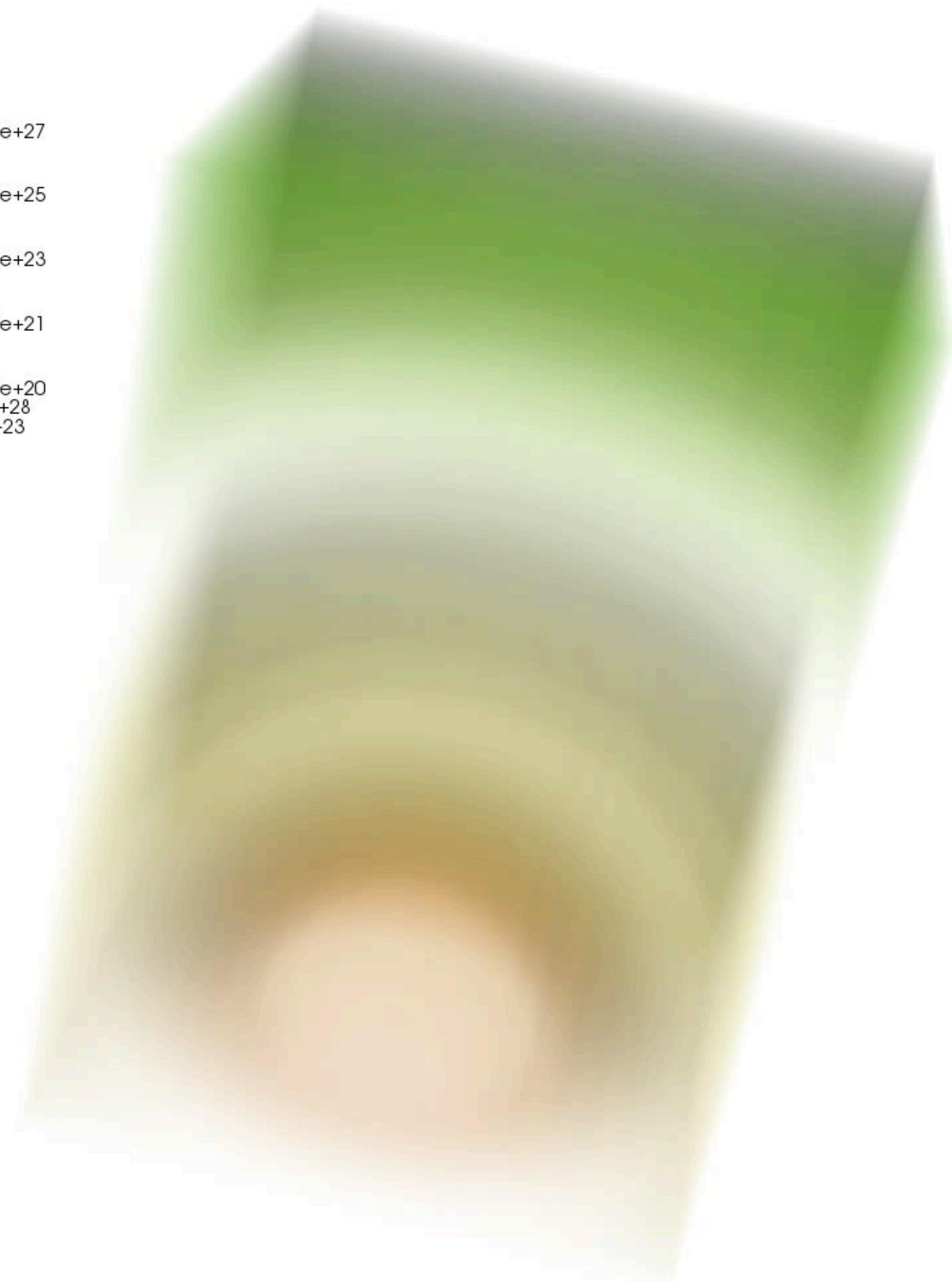


Urrutia, De Colle & Lopez-Camara 2023

Jets initially structured

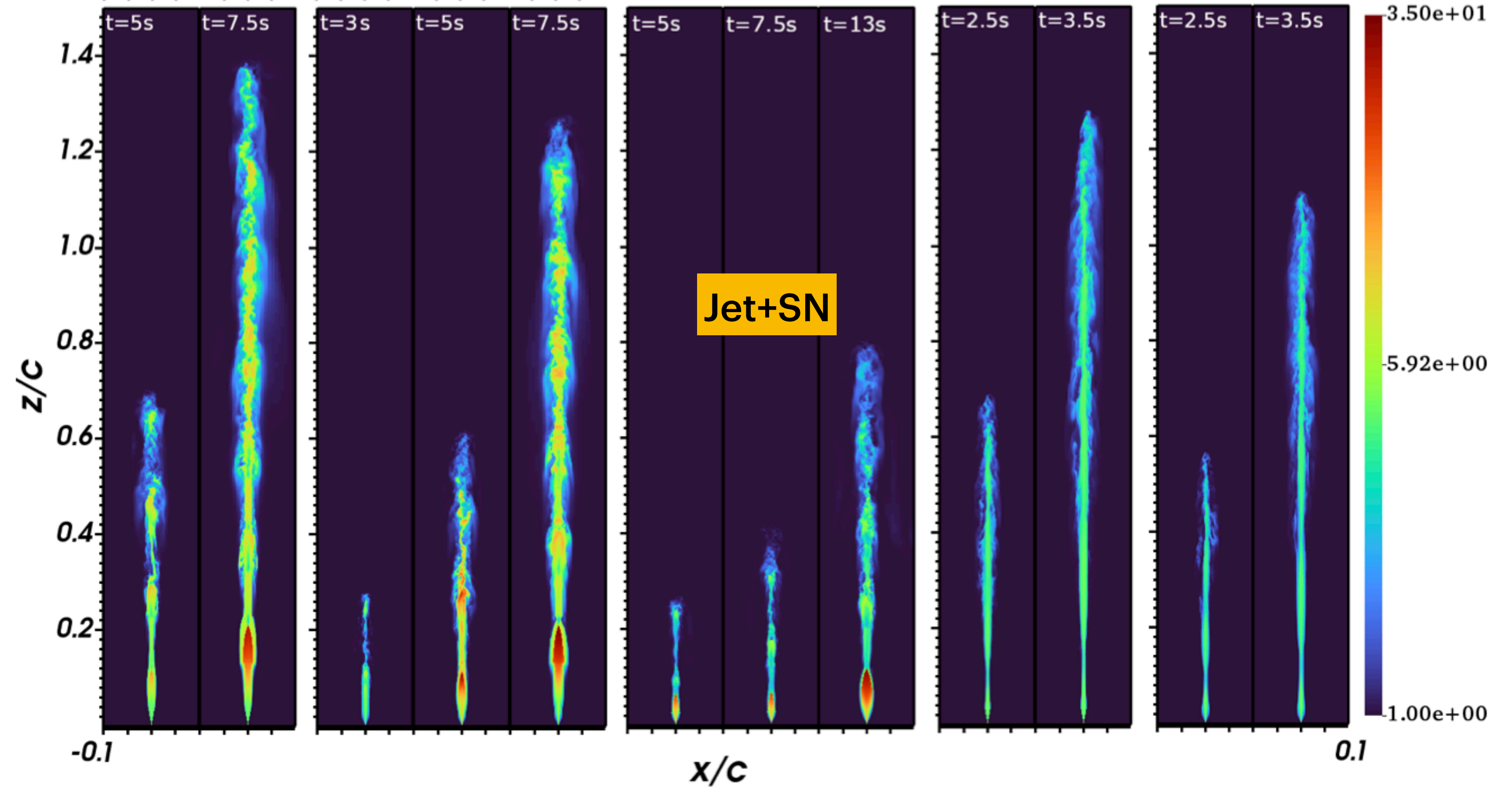
Gaussian jet + Supernova

Volume
Var: de
2.000e+27
2.991e+25
4.472e+23
6.687e+21
1.000e+20
Max: 3.718e+28
Min: 4.239e+23



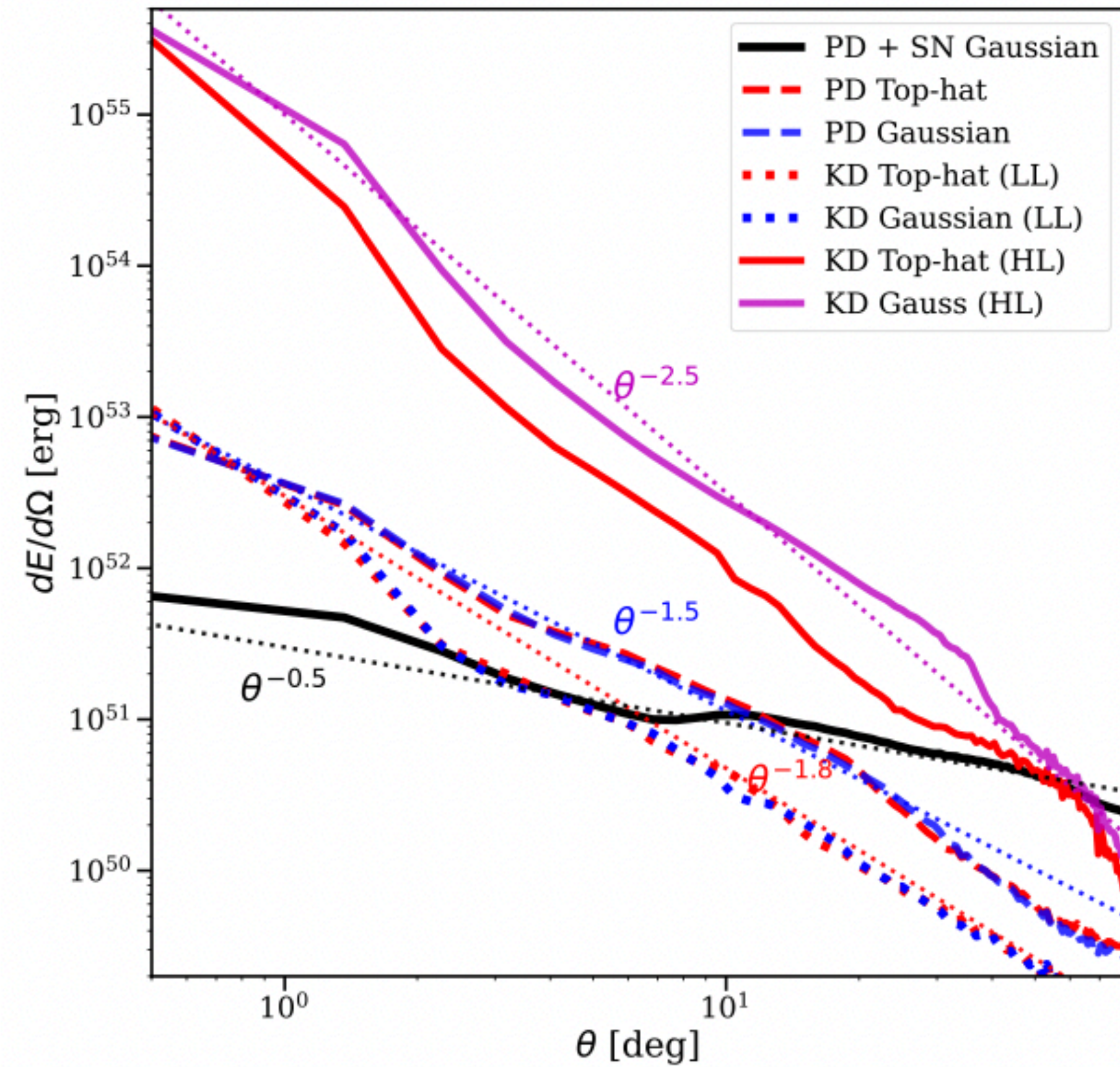
Pressure dominated

Kinetic Dominated

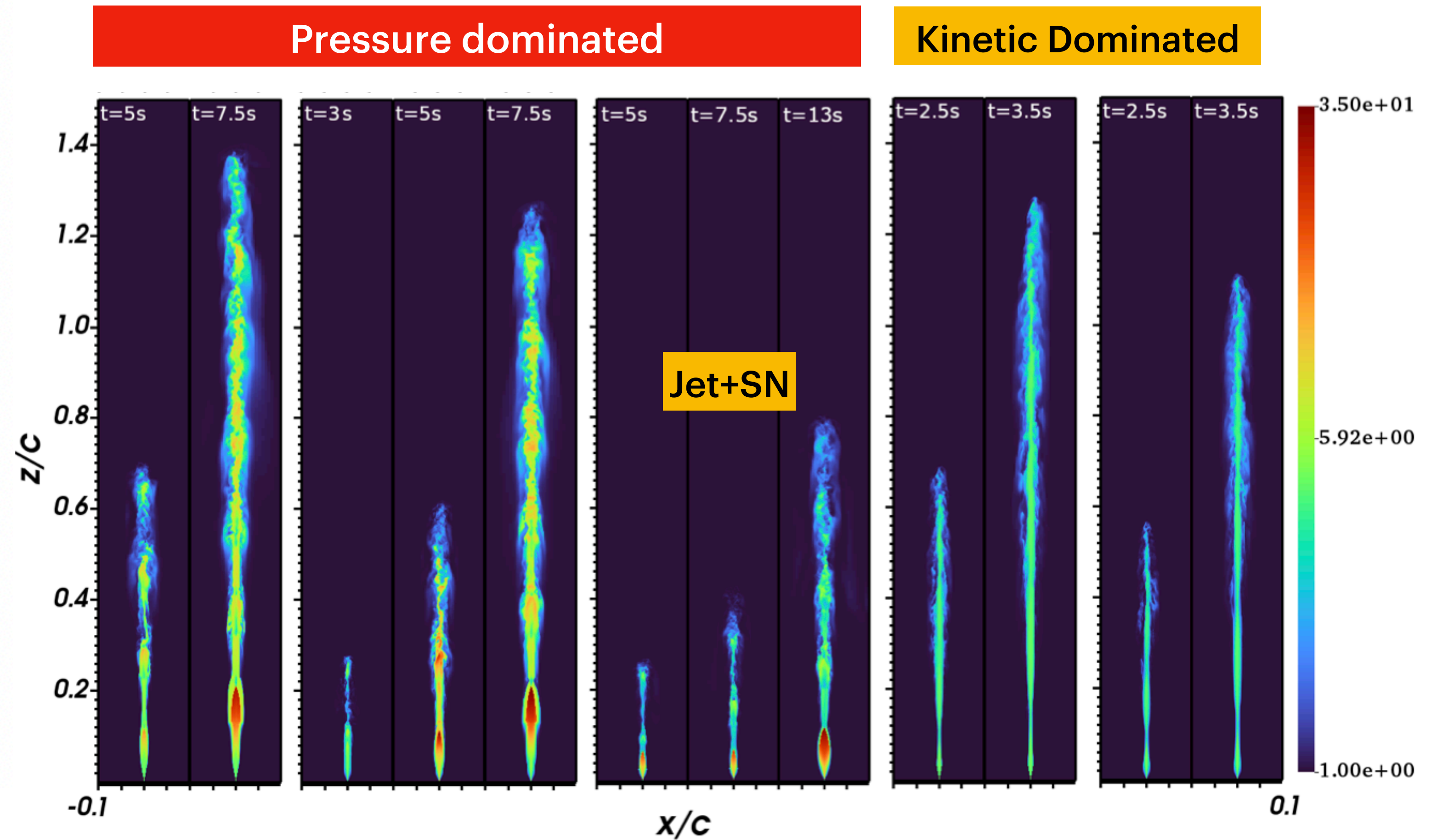


Urrutia, De Colle & Lopez-Camara 2023

Jets initially structured

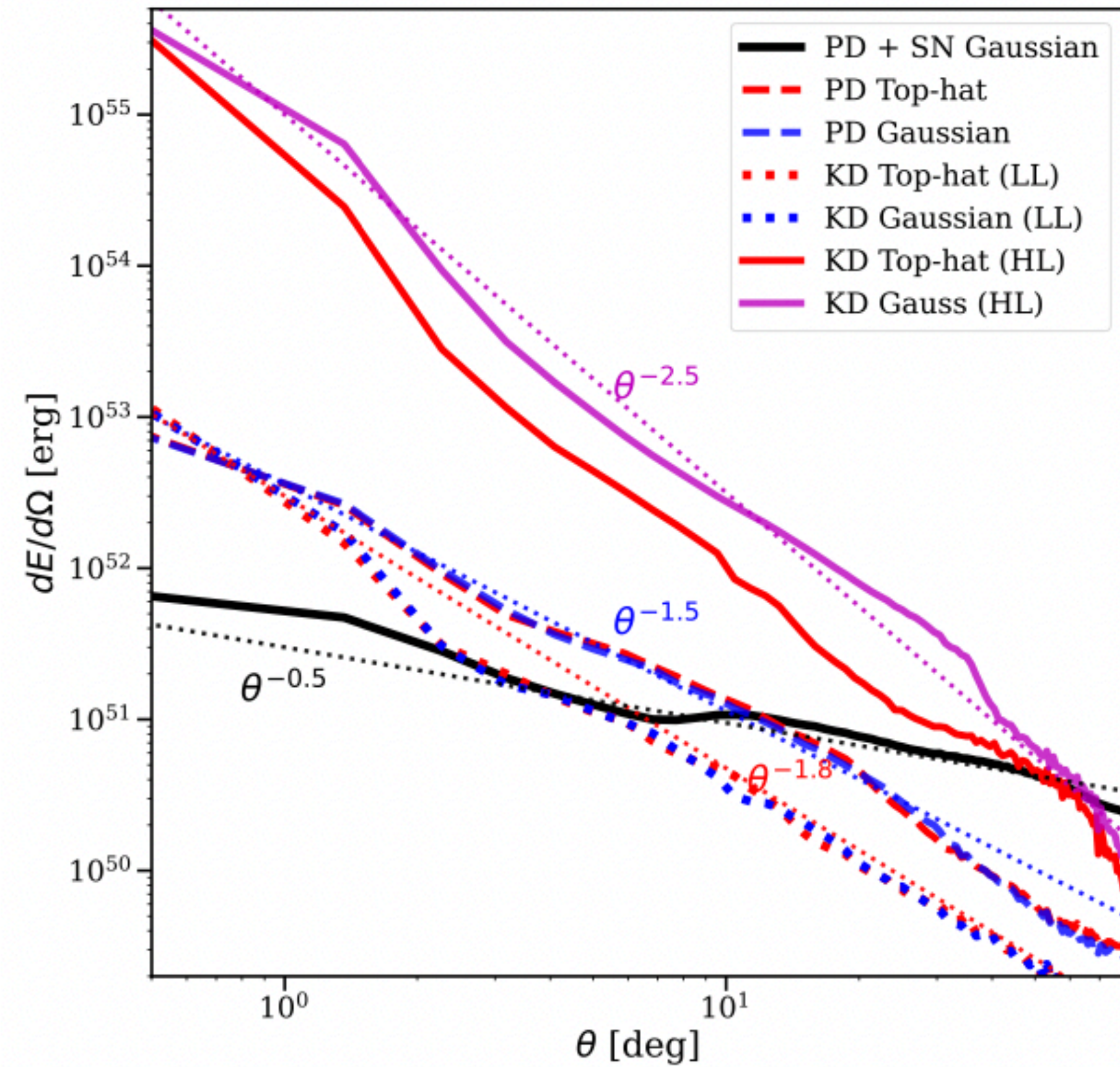


Time=0

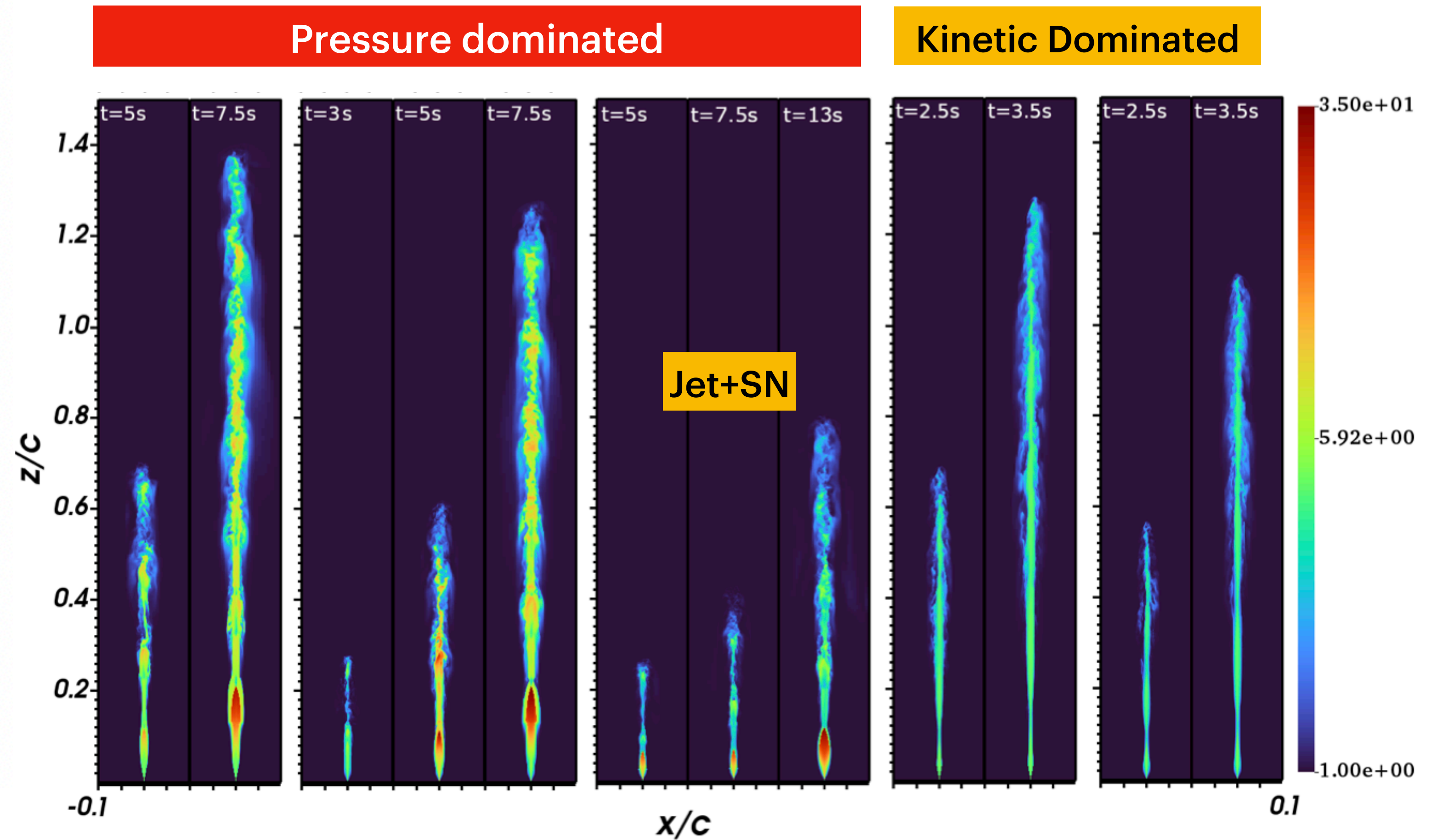


Urrutia, De Colle & Lopez-Camara 2023

Jets initially structured

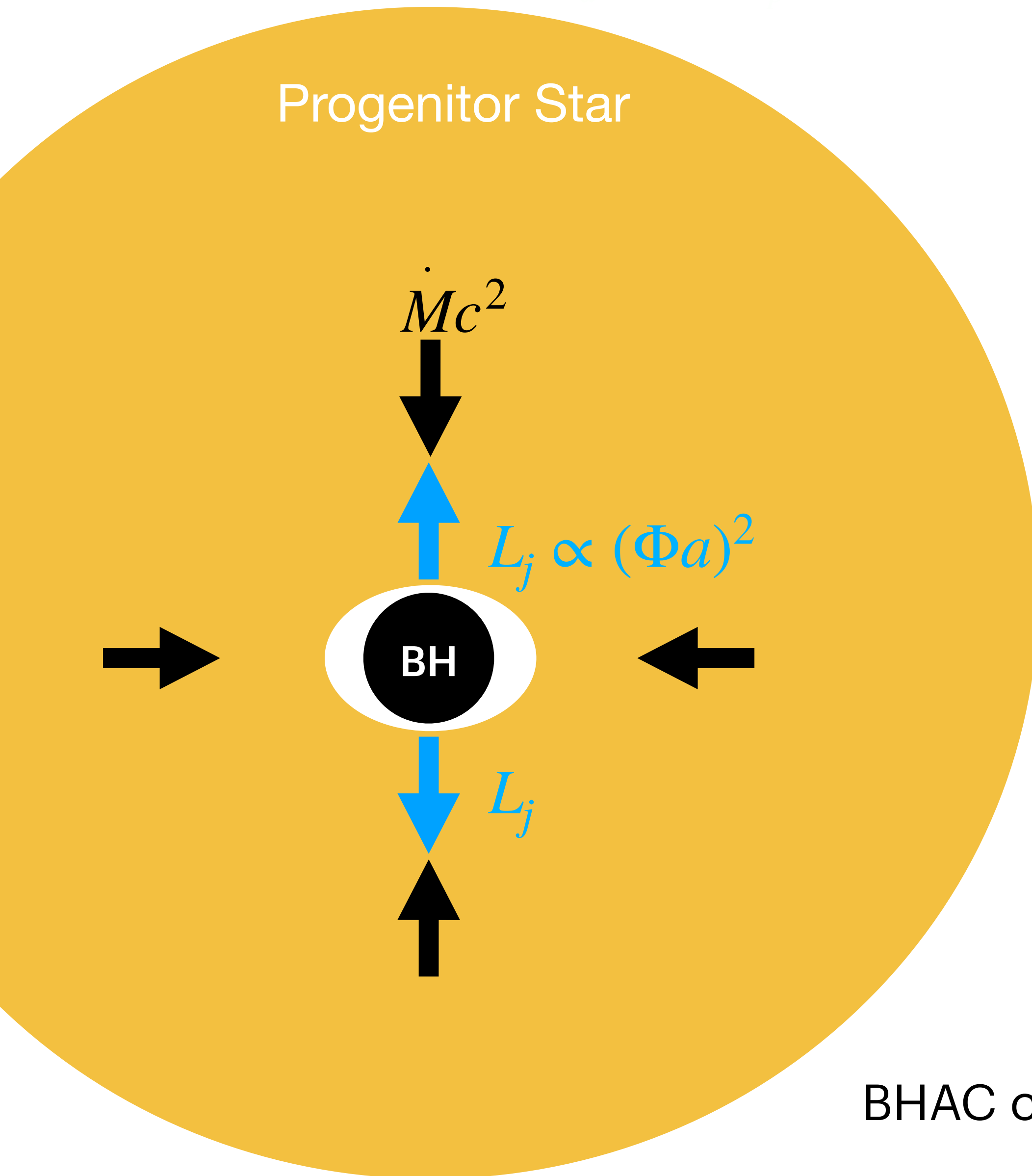


Time=0



Urrutia, De Colle & Lopez-Camara 2023

Simulations from small scales



Rotation

$$\epsilon_{\text{isco}} = -u_{t,\text{isco}} = \frac{1 - 2/r_{\text{isco}} + a/r_{\text{isco}}^{3/2}}{\sqrt{1 - 3/r_{\text{isco}} + 2a/r_{\text{isco}}^{3/2}}}$$

$$l_{\text{isco}} = u_{\phi,\text{isco}} = \frac{r_{\text{isco}}^{1/2} - 2a/r_{\text{isco}} + a^2/r_{\text{isco}}^{3/2}}{\sqrt{1 - 3/r_{\text{isco}} + 2a/r_{\text{isco}}^{3/2}}}$$

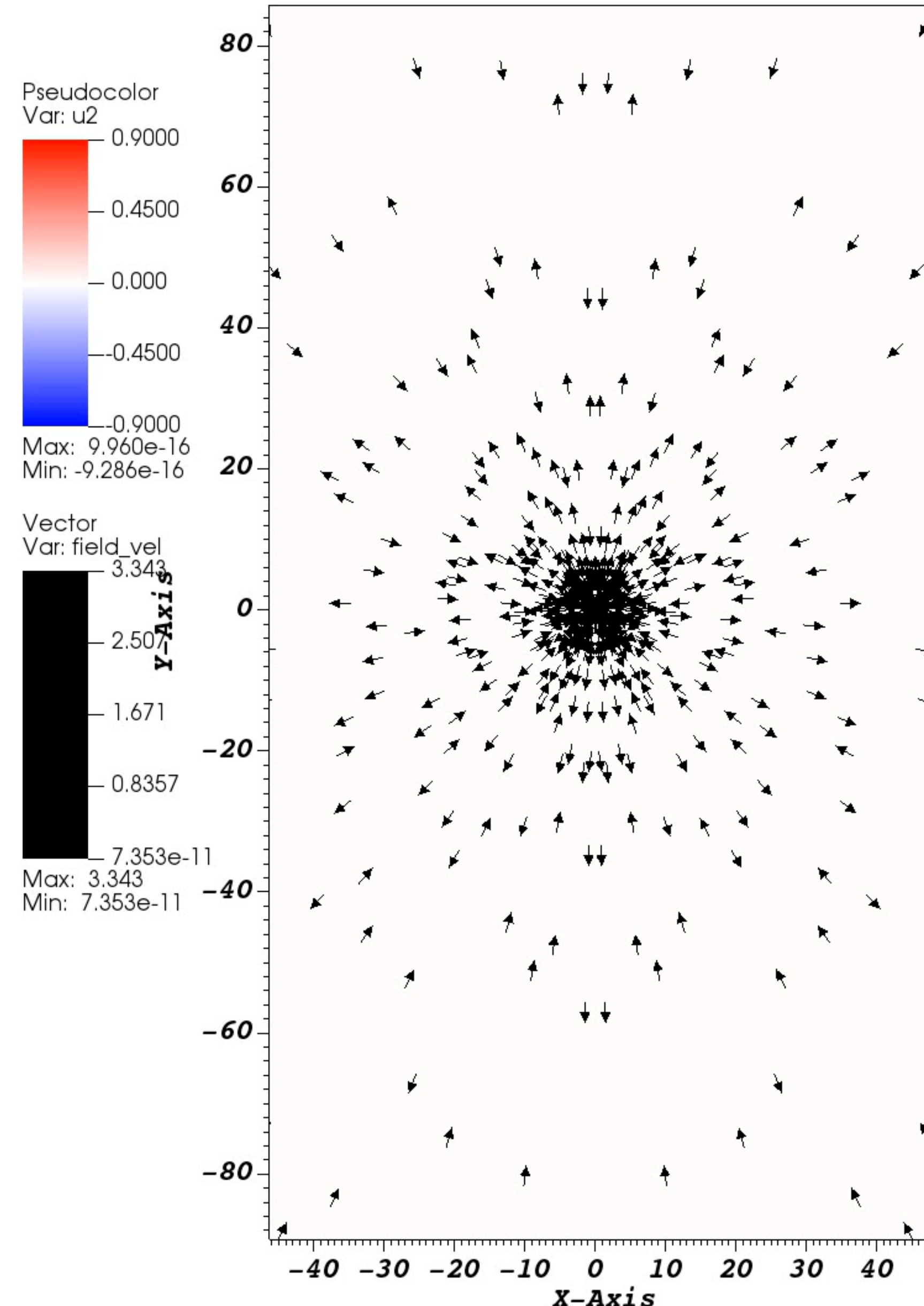
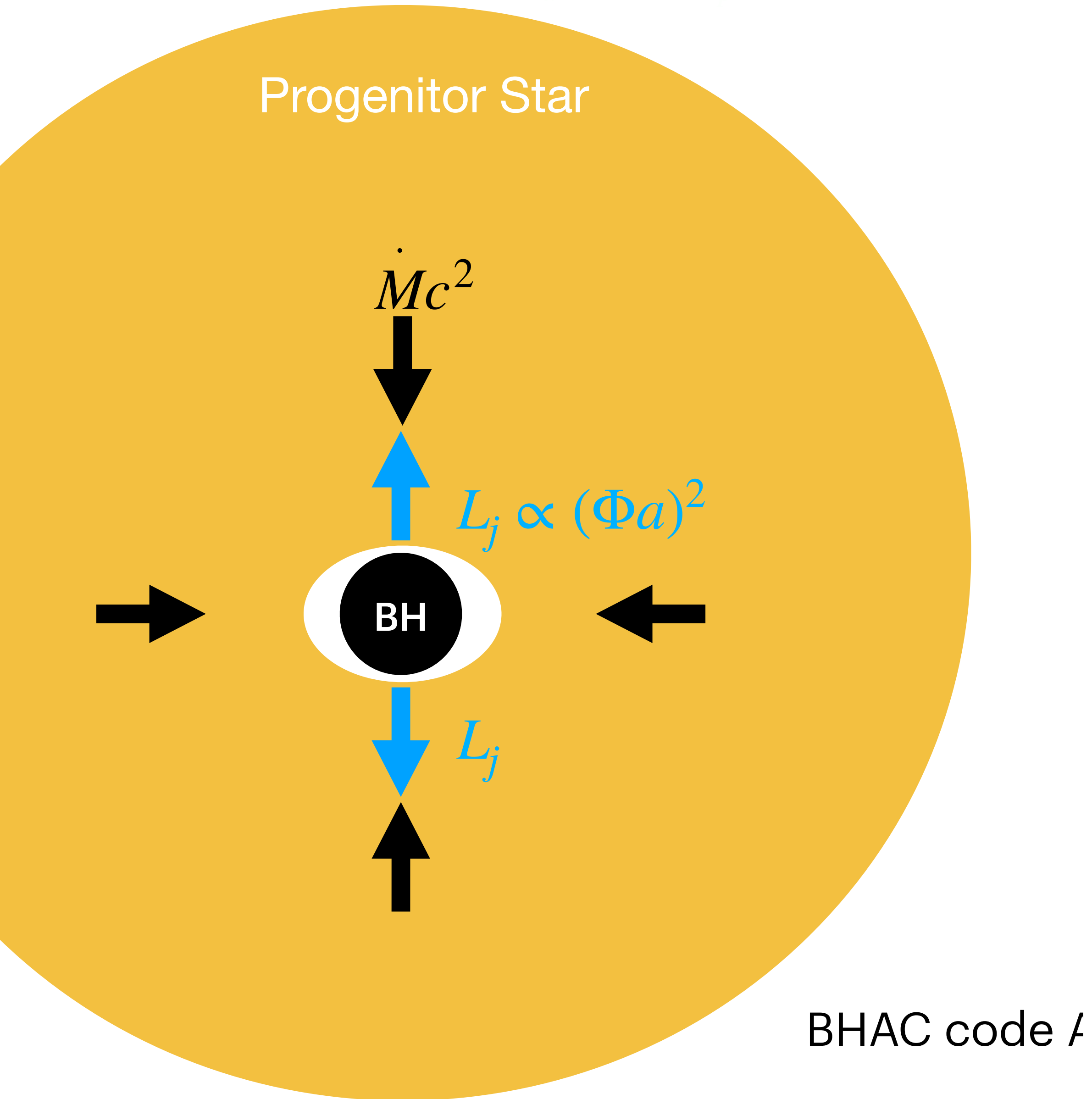
$$u^\phi = C \sin^2 \theta (-g^{t\phi} \epsilon_{\text{isco}} + g^{\phi\phi} l_{\text{isco}})$$

Magnetic Field Potential

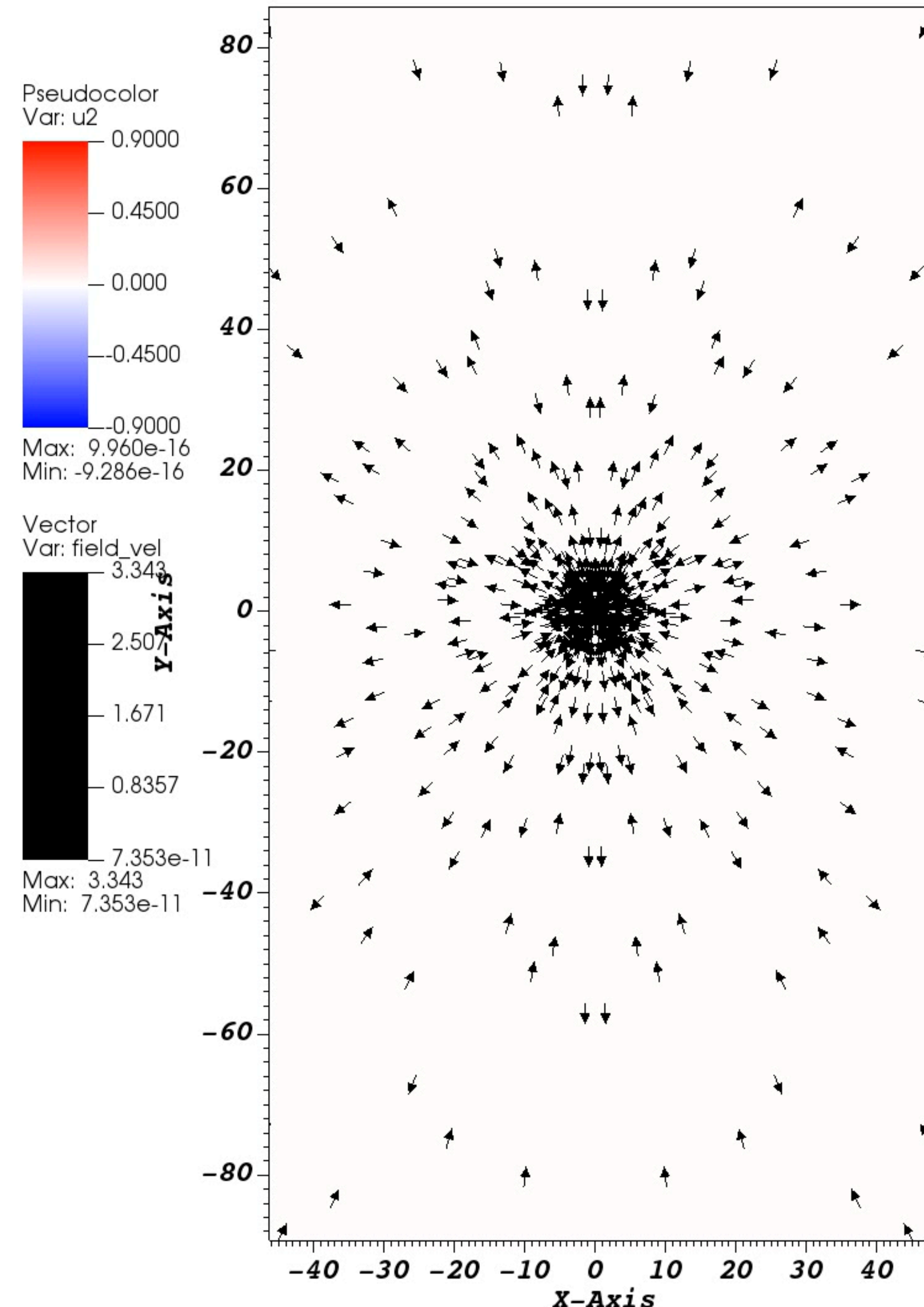
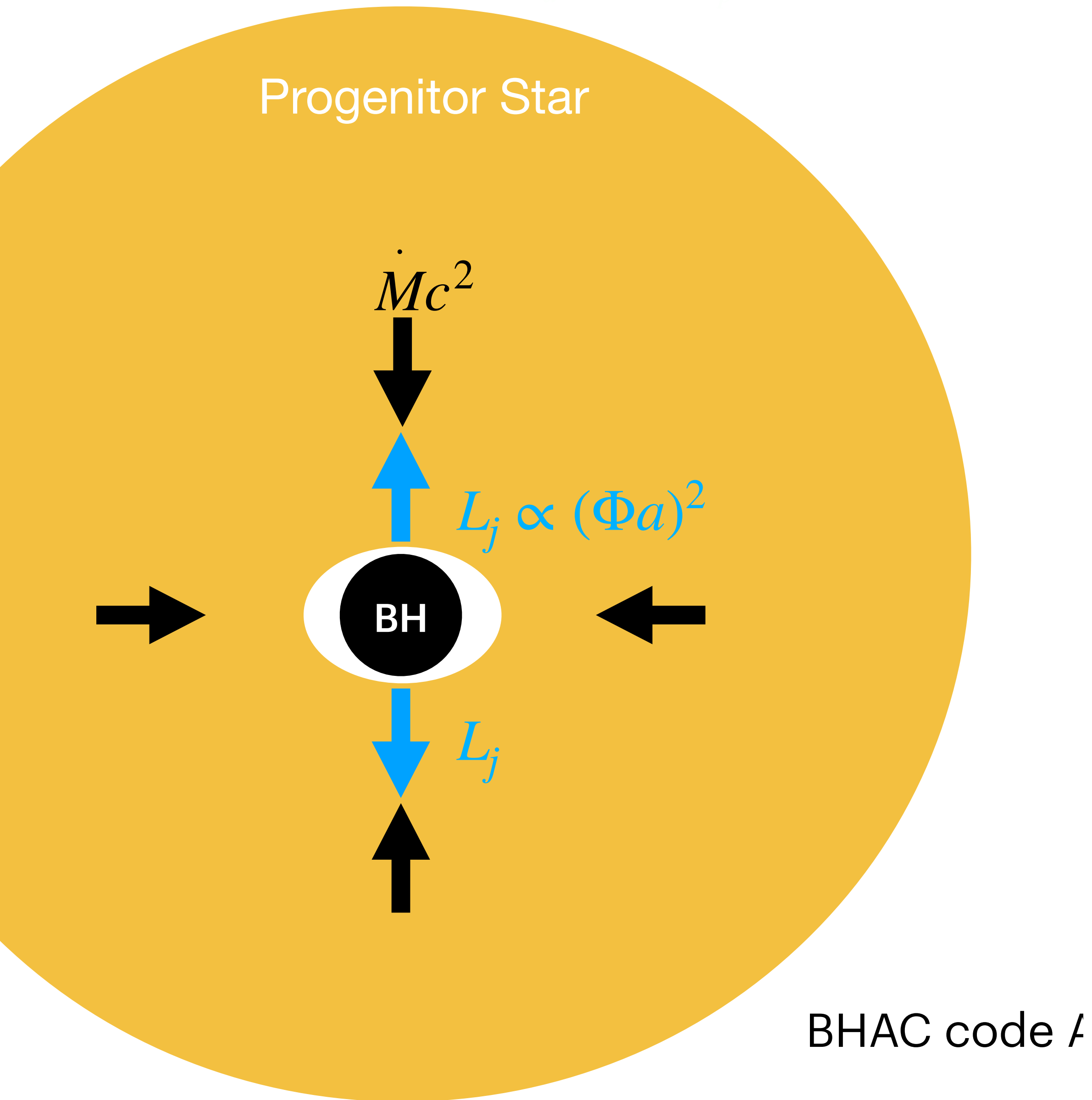
$$A_\phi = \frac{B_0 r_c^3}{r^3 + r_0^3} \sin \theta$$

$$B_0 = 10^{14}$$

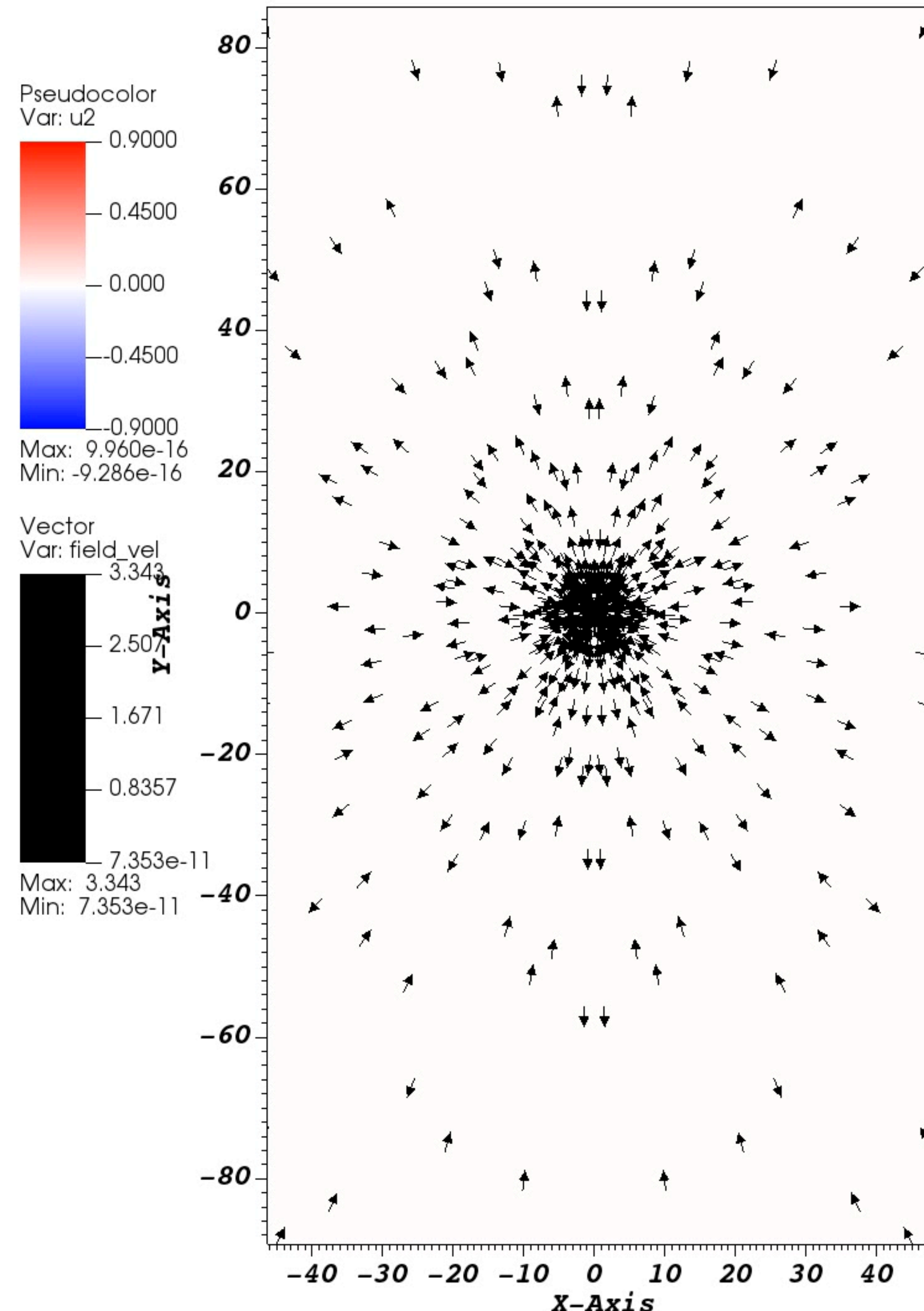
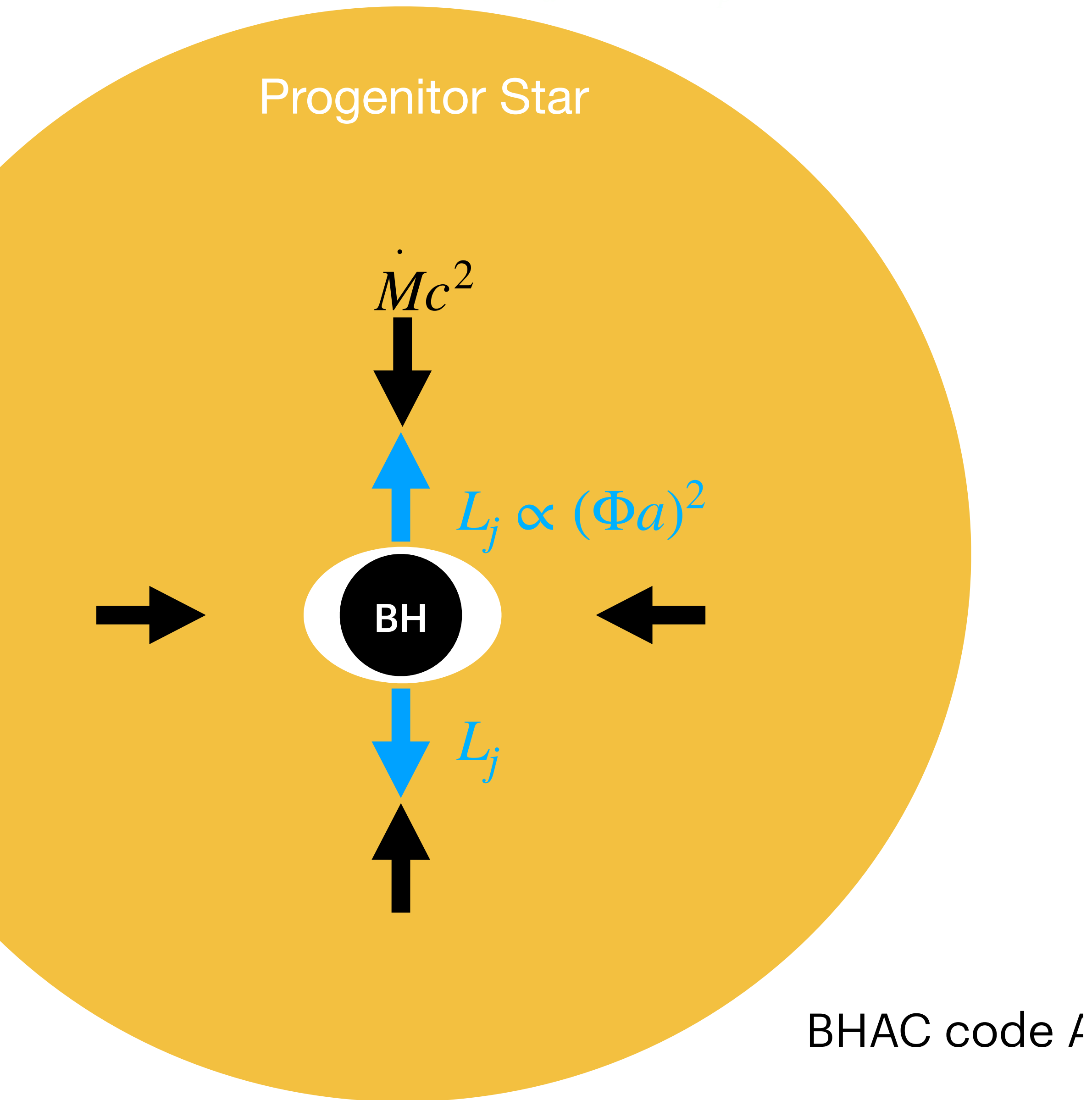
Simulations from small scales



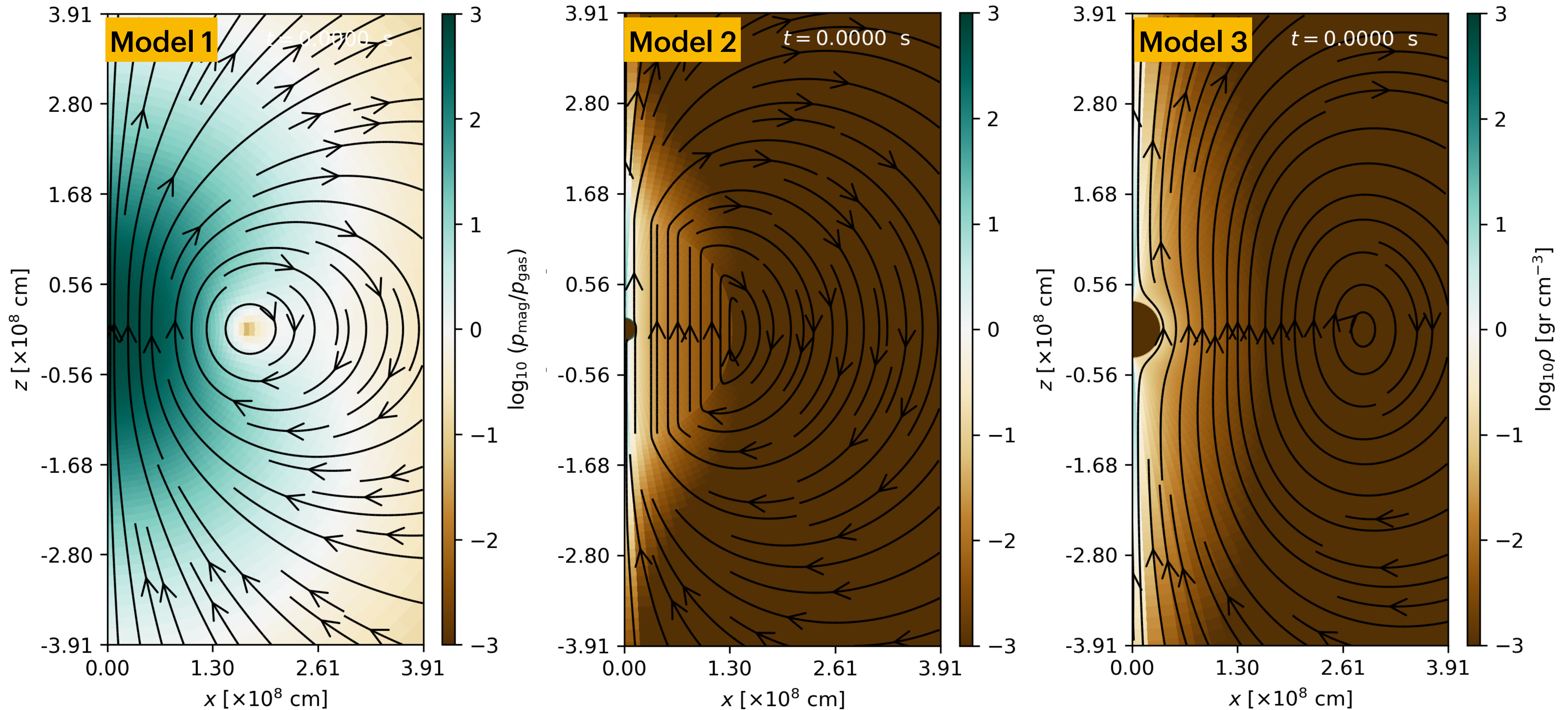
Simulations from small scales



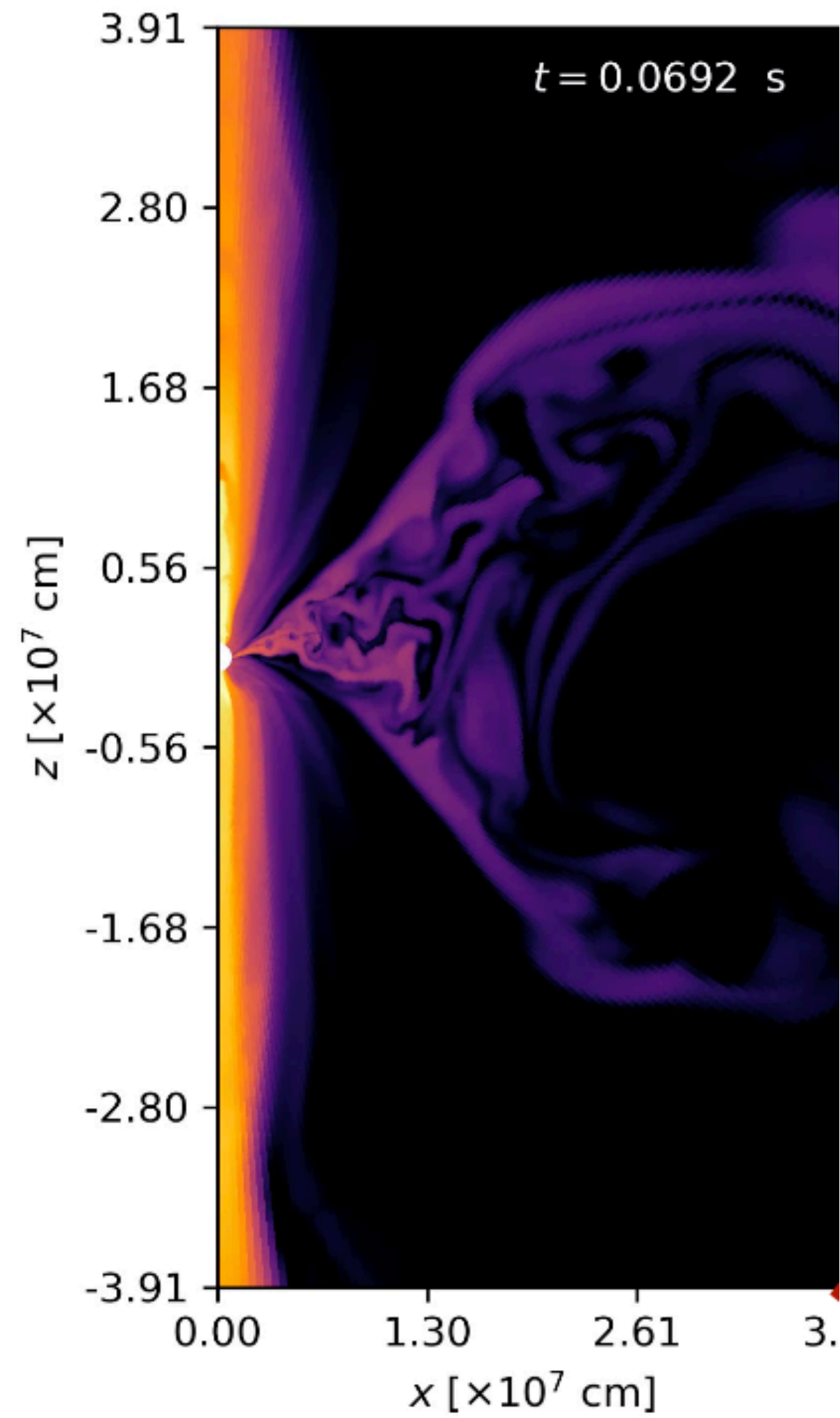
Simulations from small scales



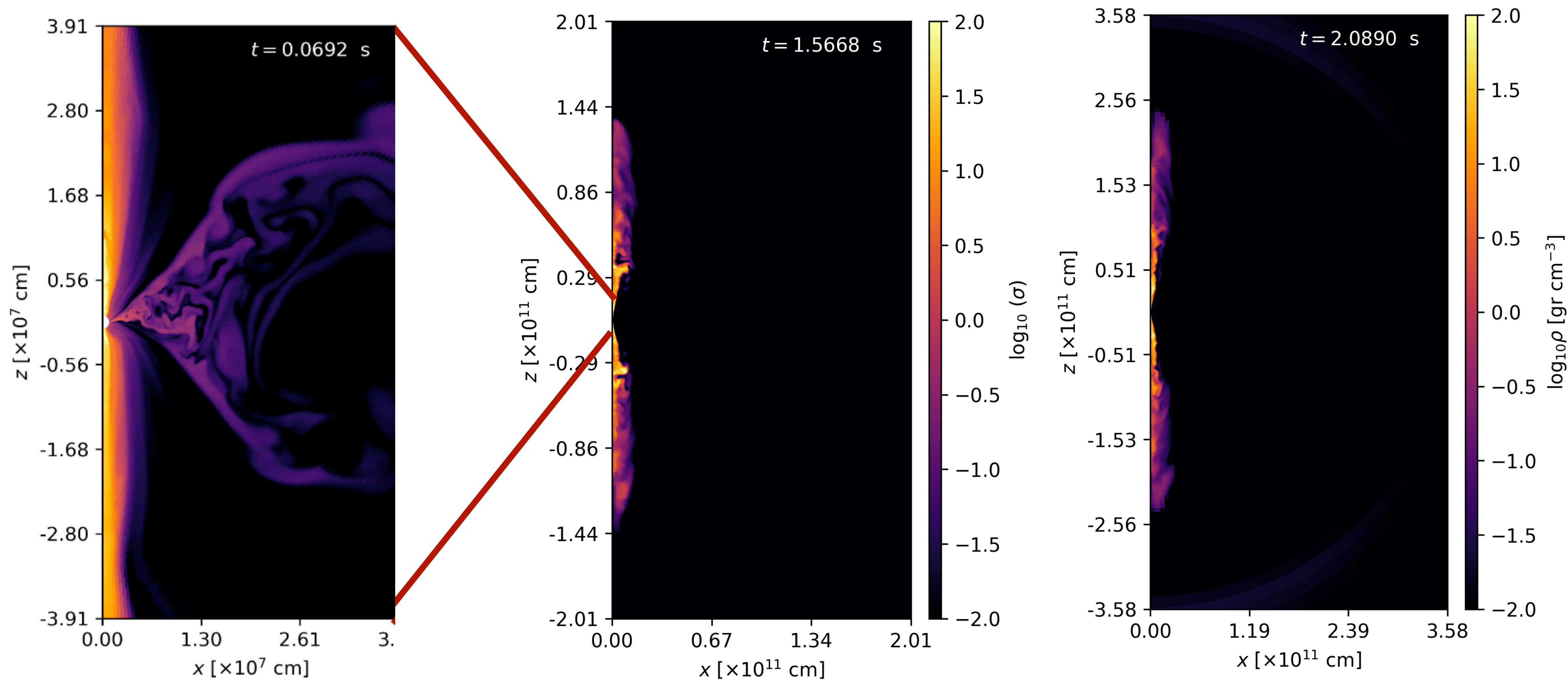
Initial magnetic field configuration



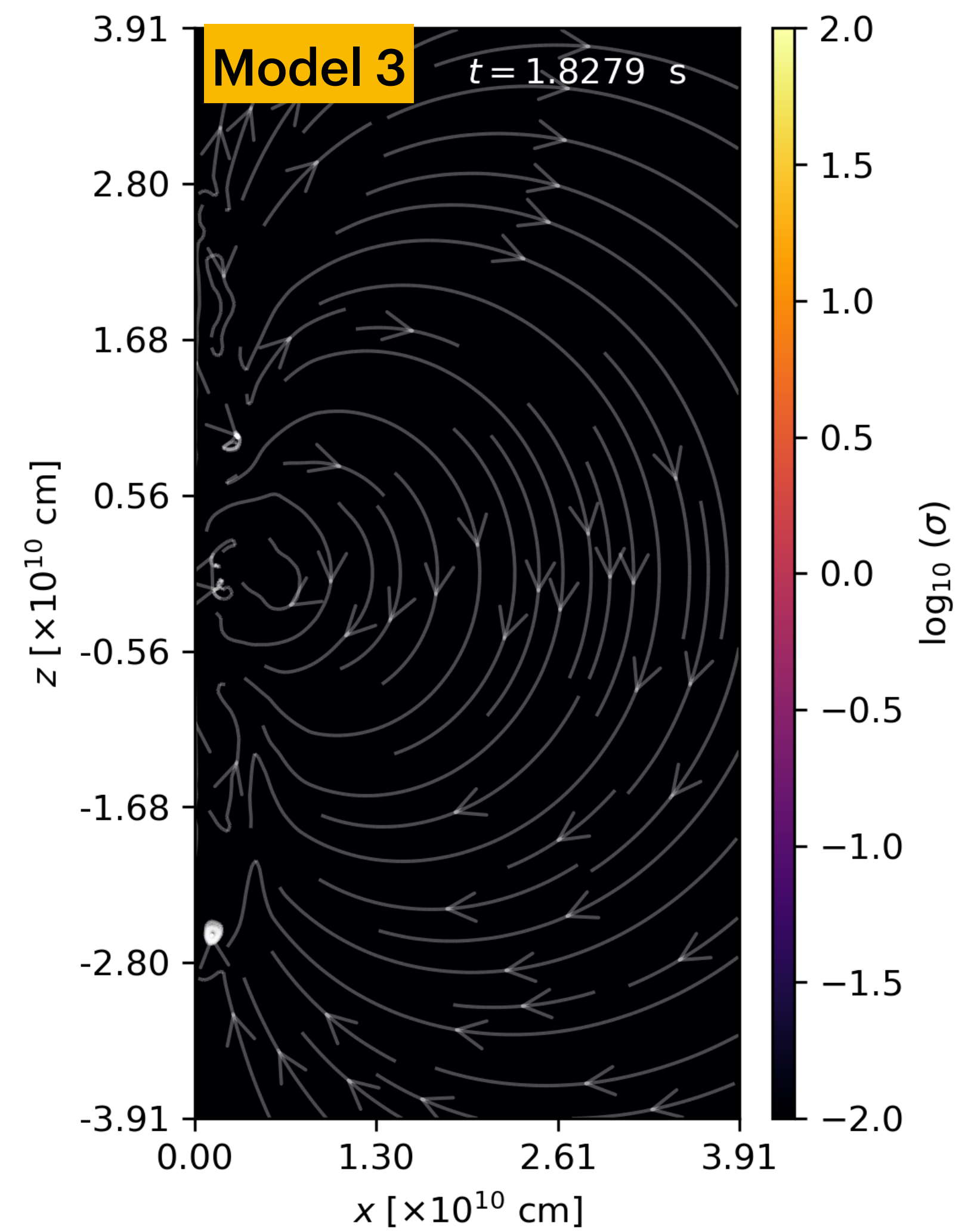
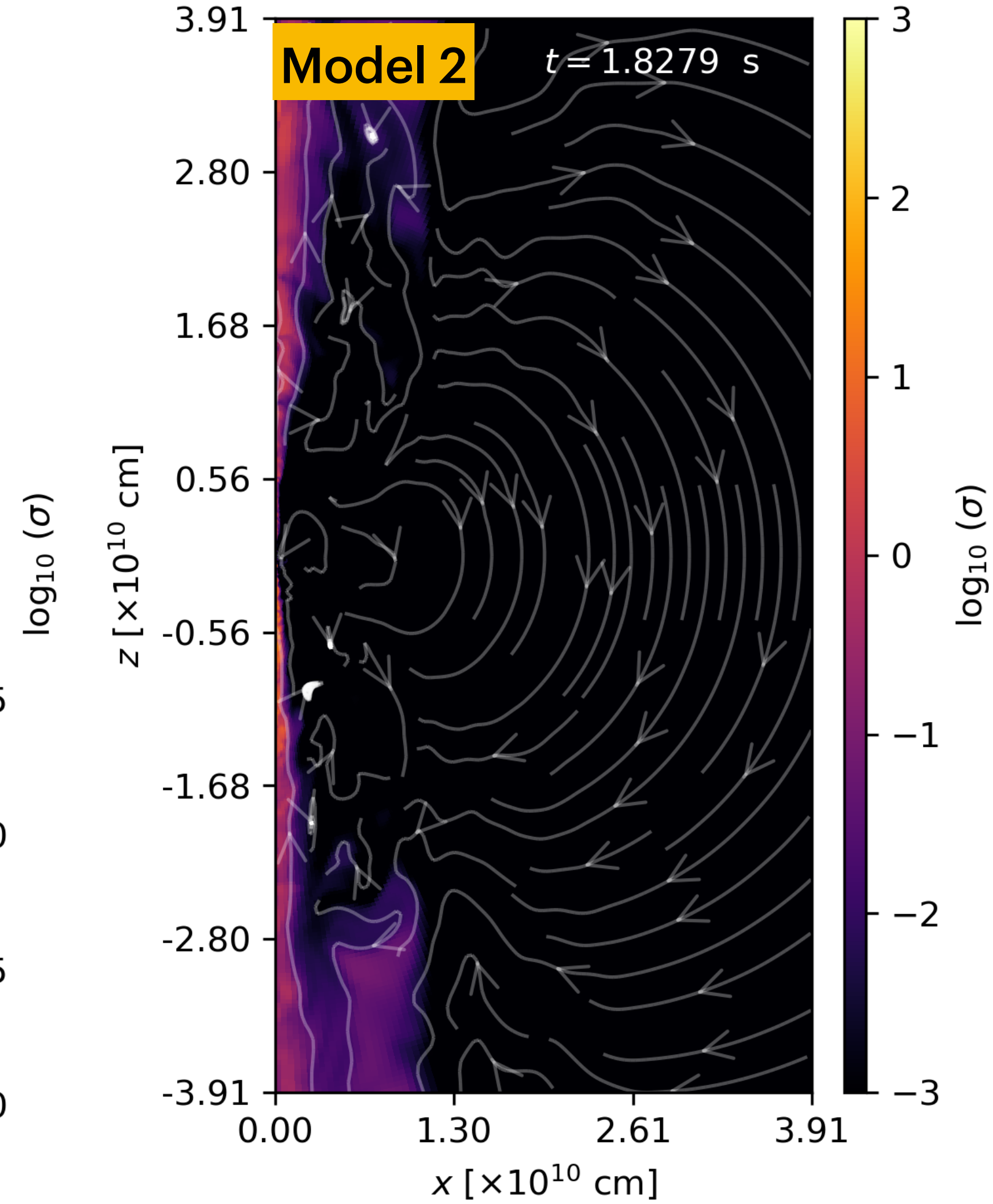
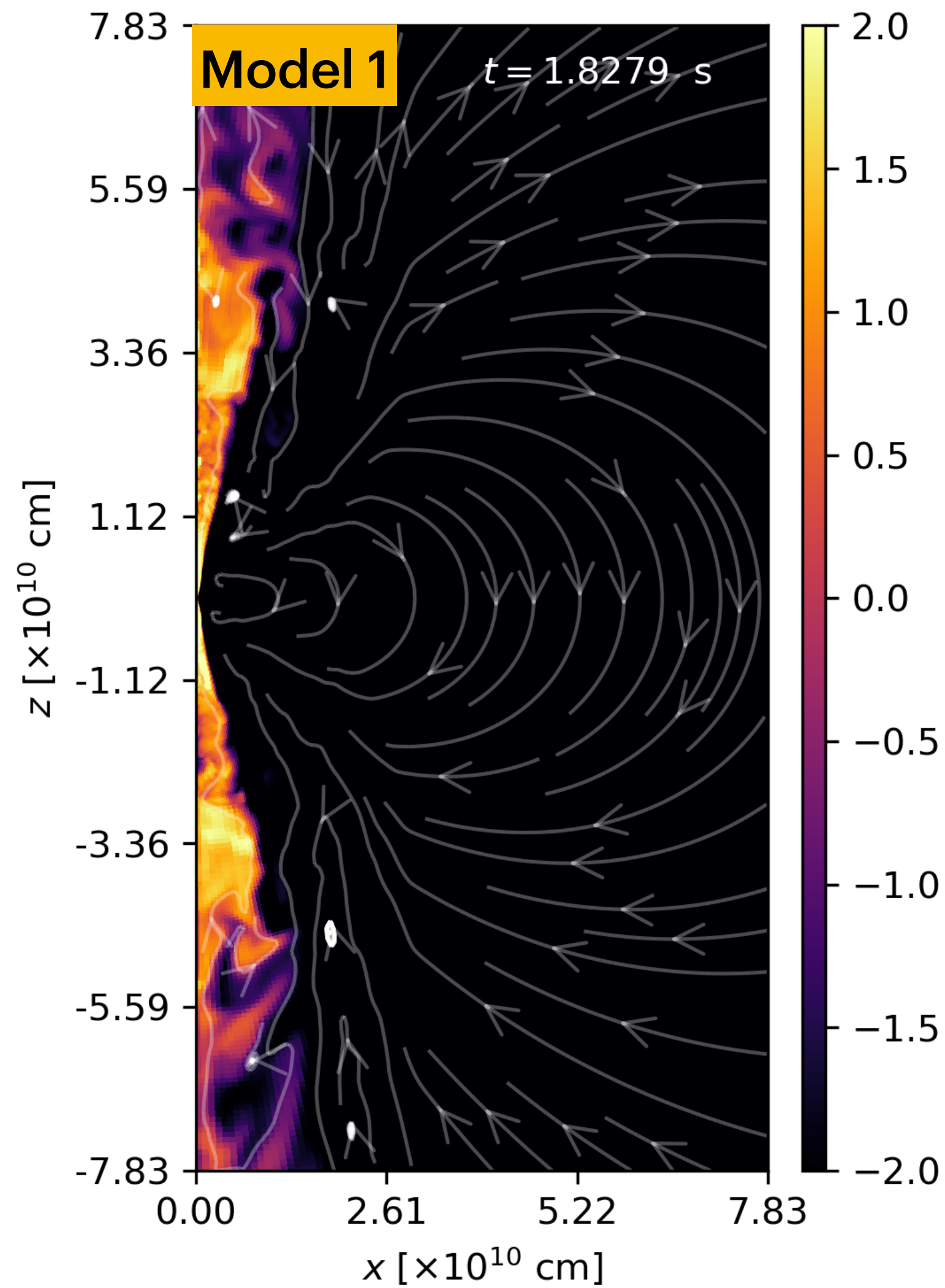
Jet launching and evolution



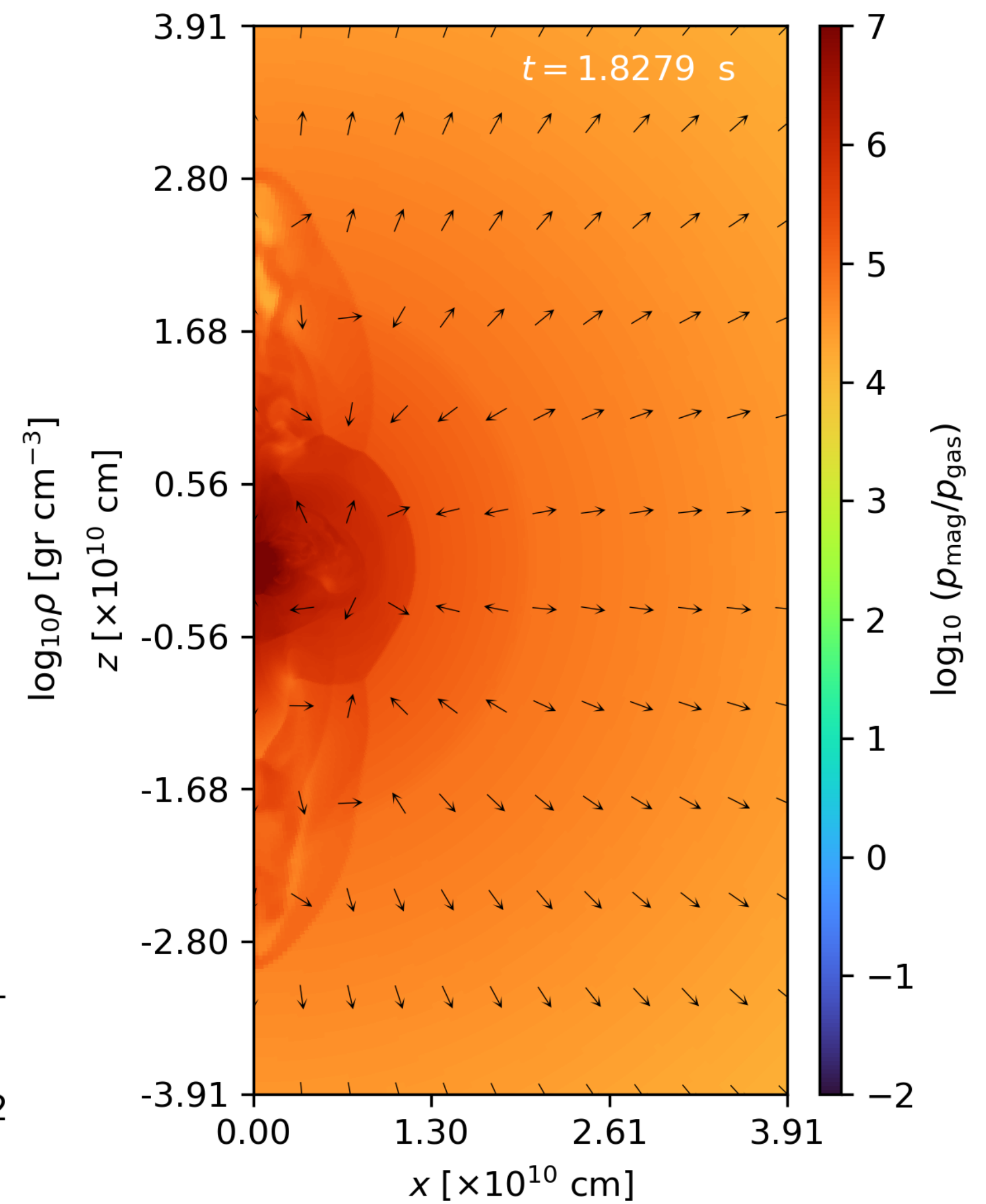
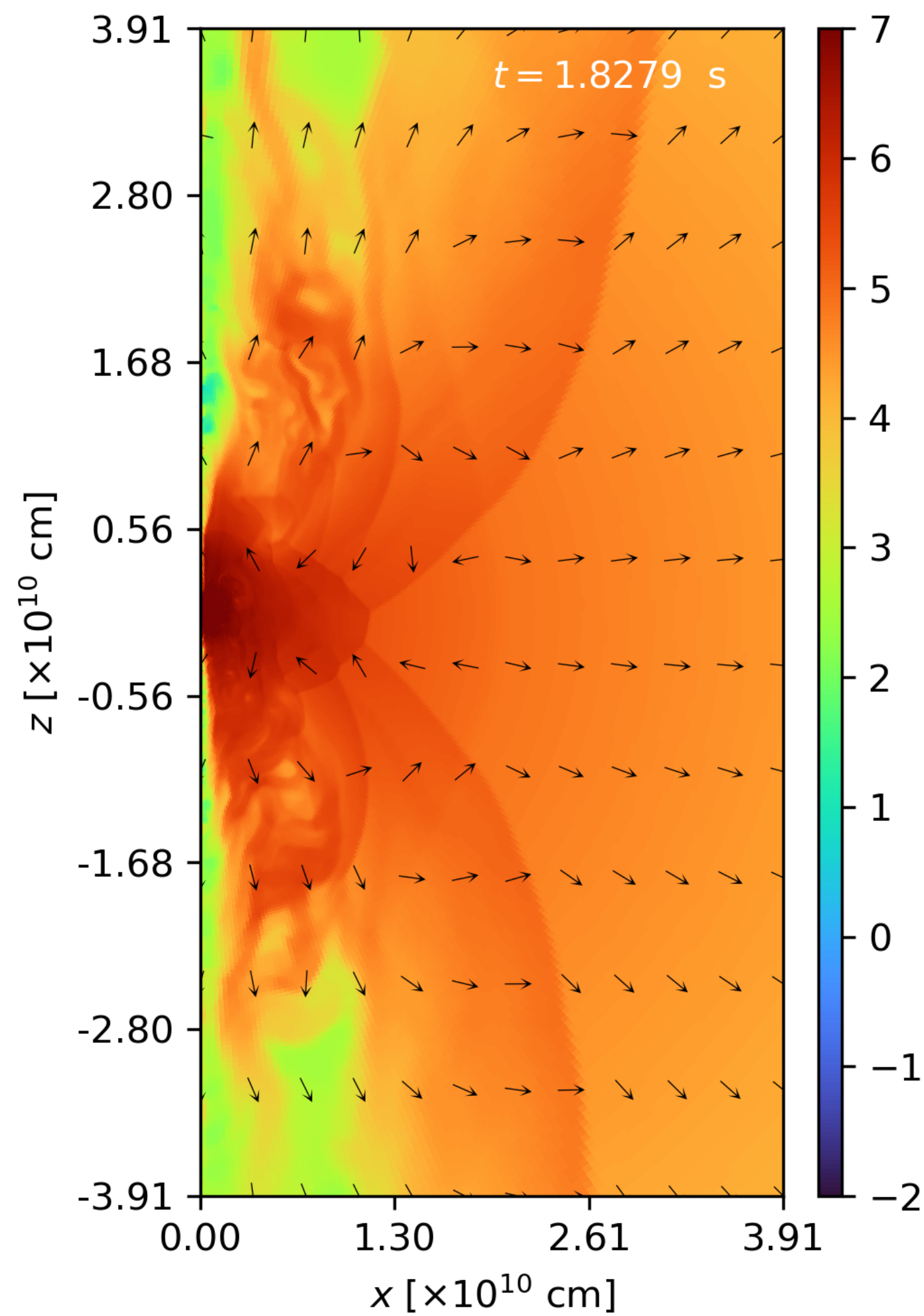
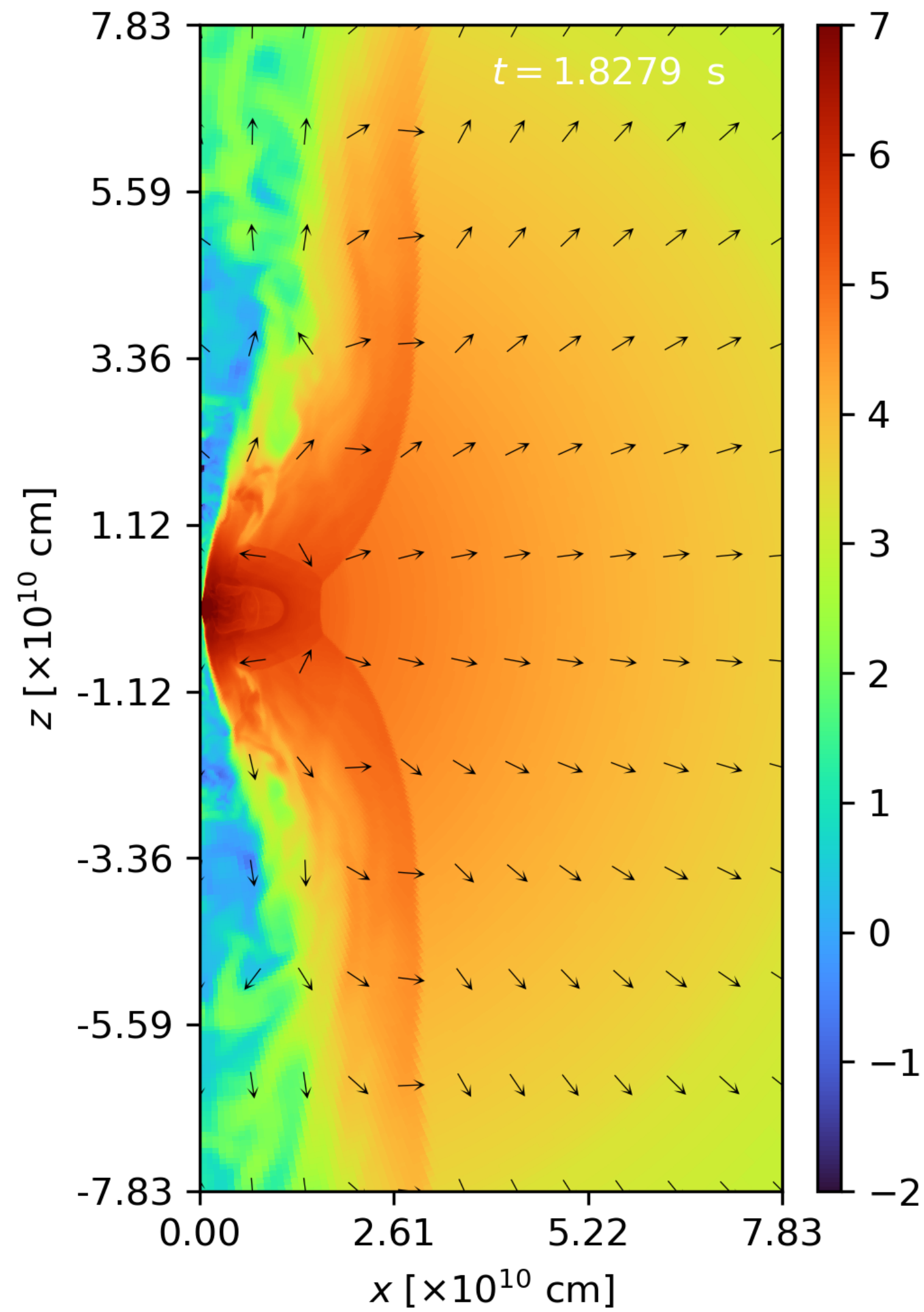
Jet launching and evolution



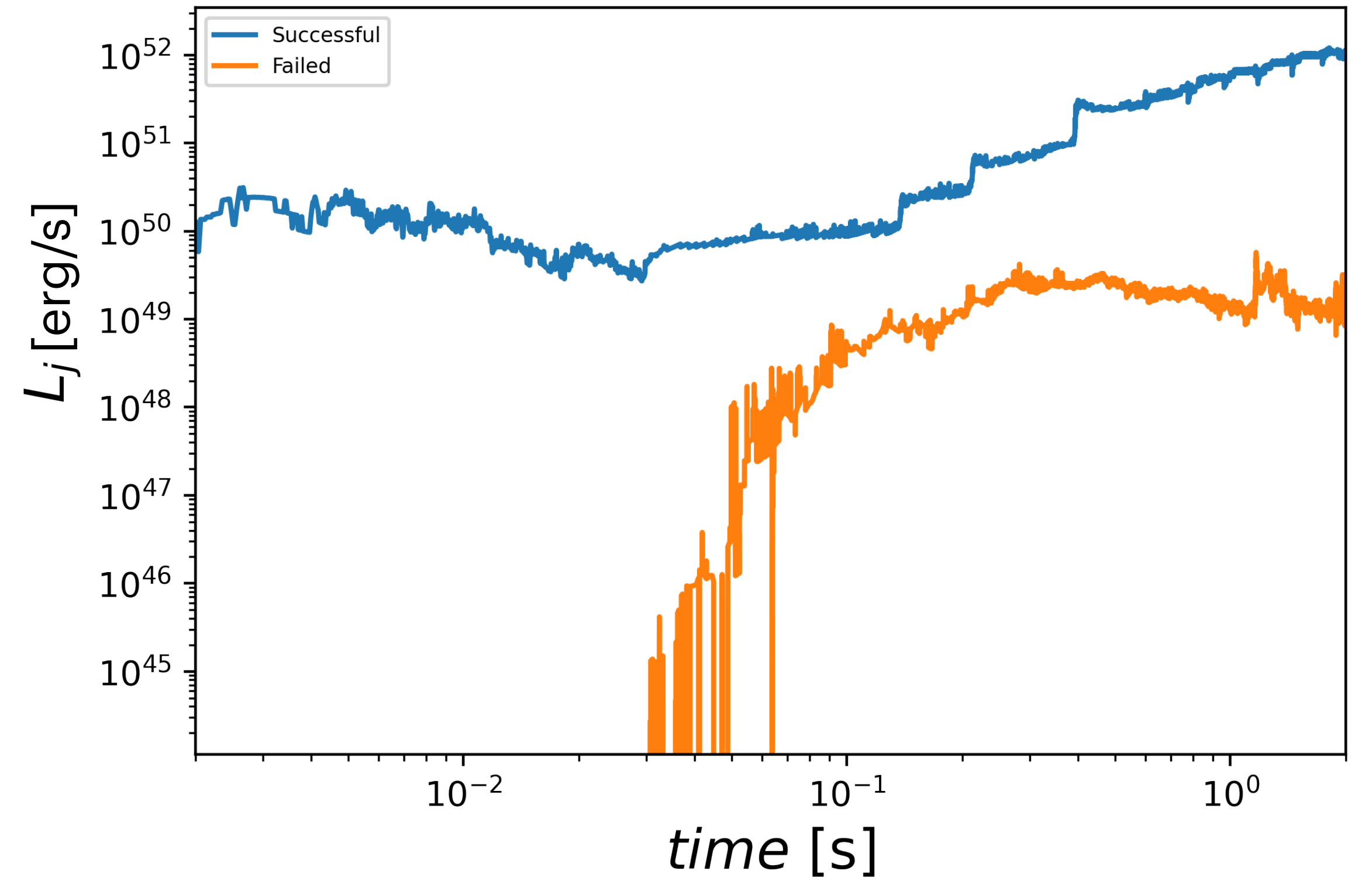
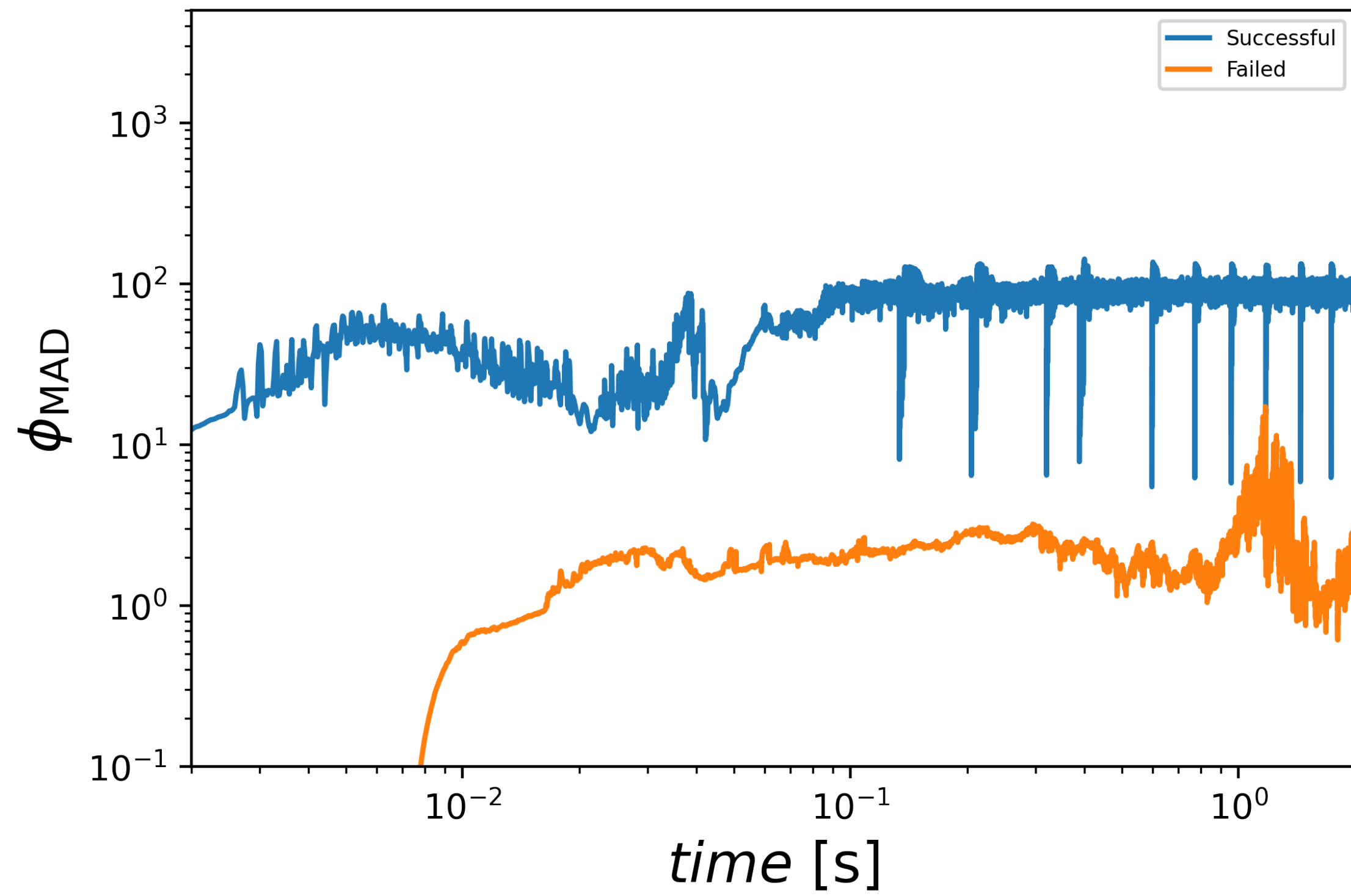
Magnetization



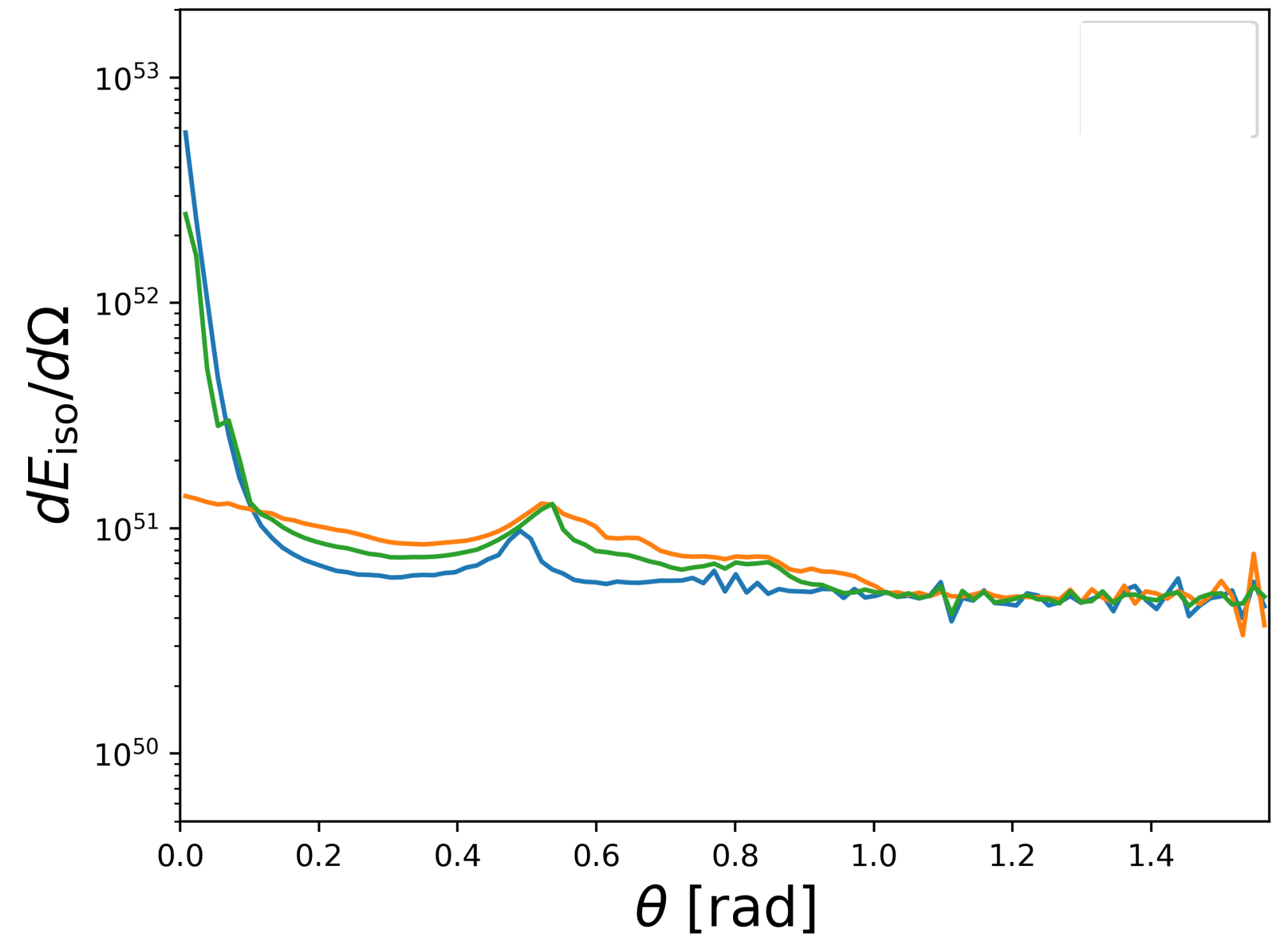
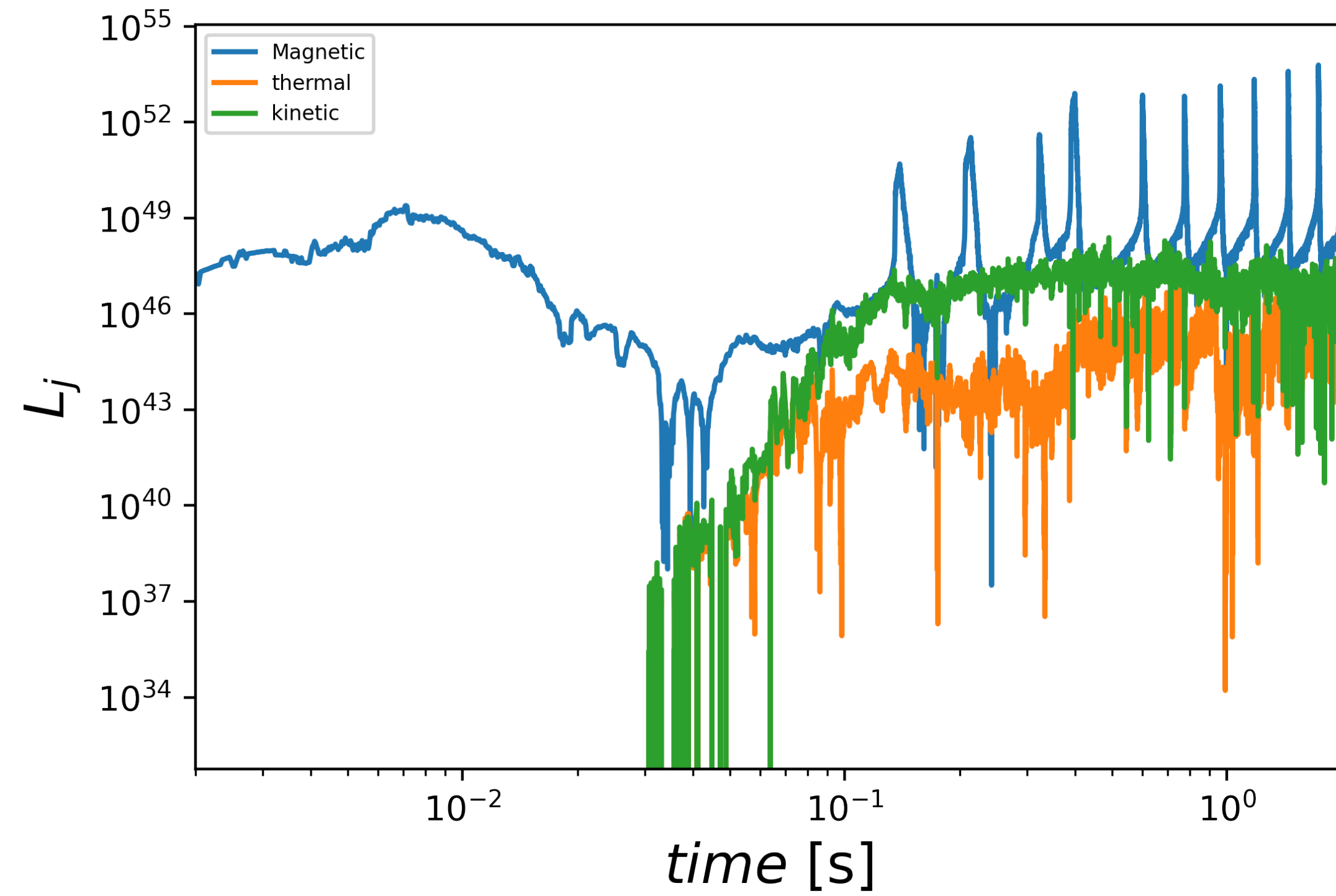
Density

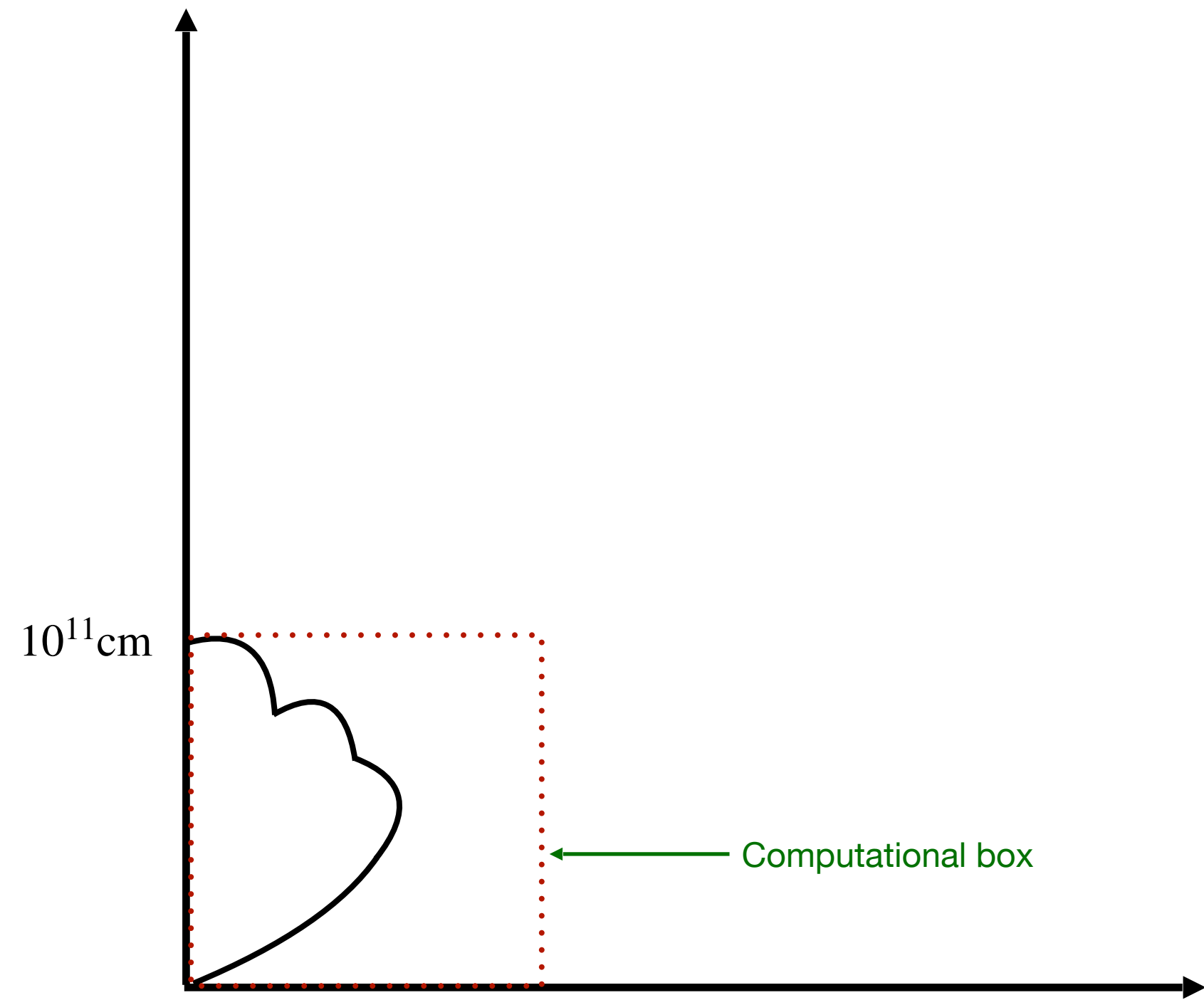


Flux evolution



Energy components and structure

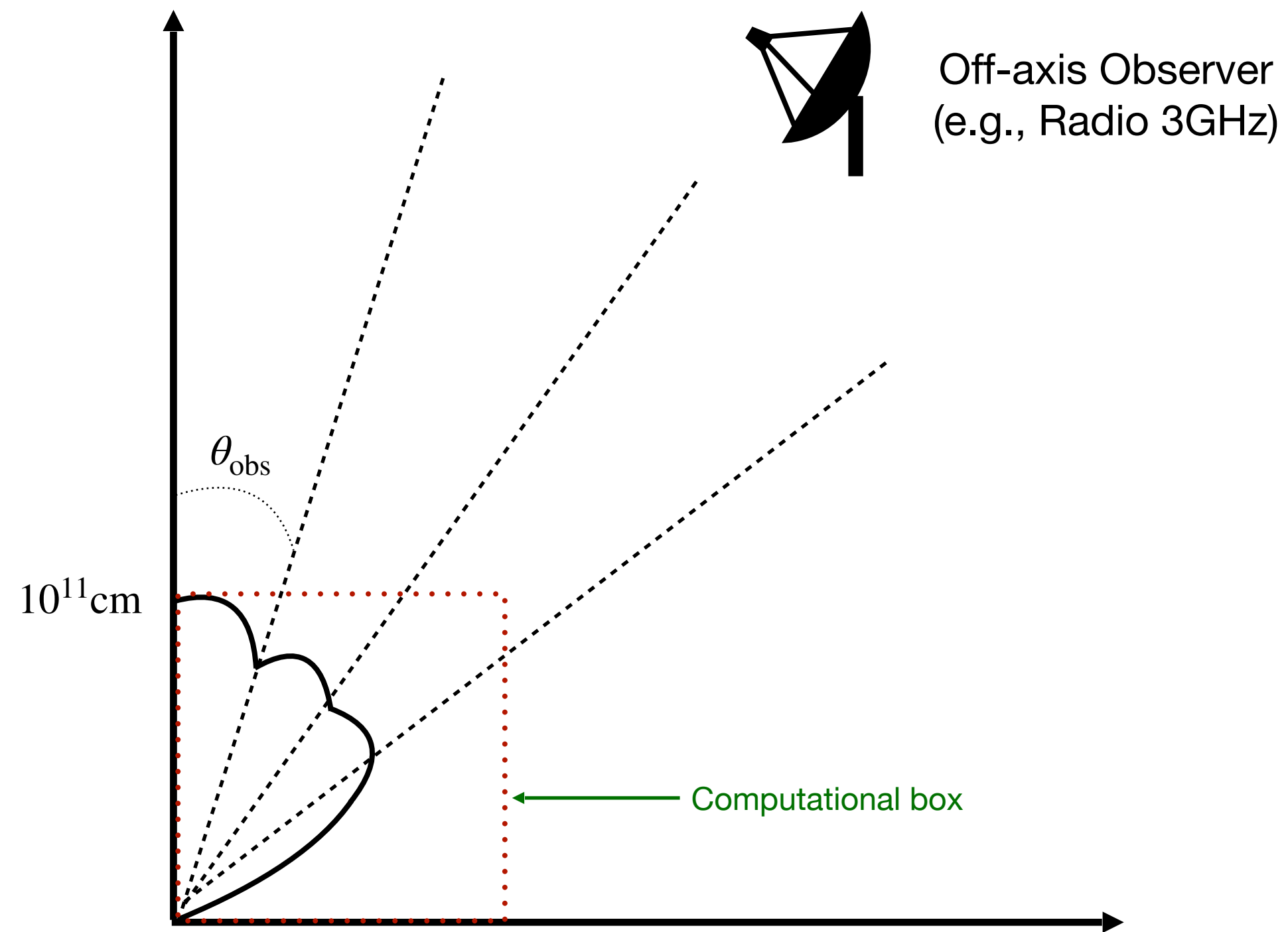




We follow the standard afterglow estimation
(Sari, Piran & Narayan 1990; Granot & Sari 2002)

- Blandford & Mckee 1976 model
- Synchrotron emission. Magnetic field amplified in the shock front.

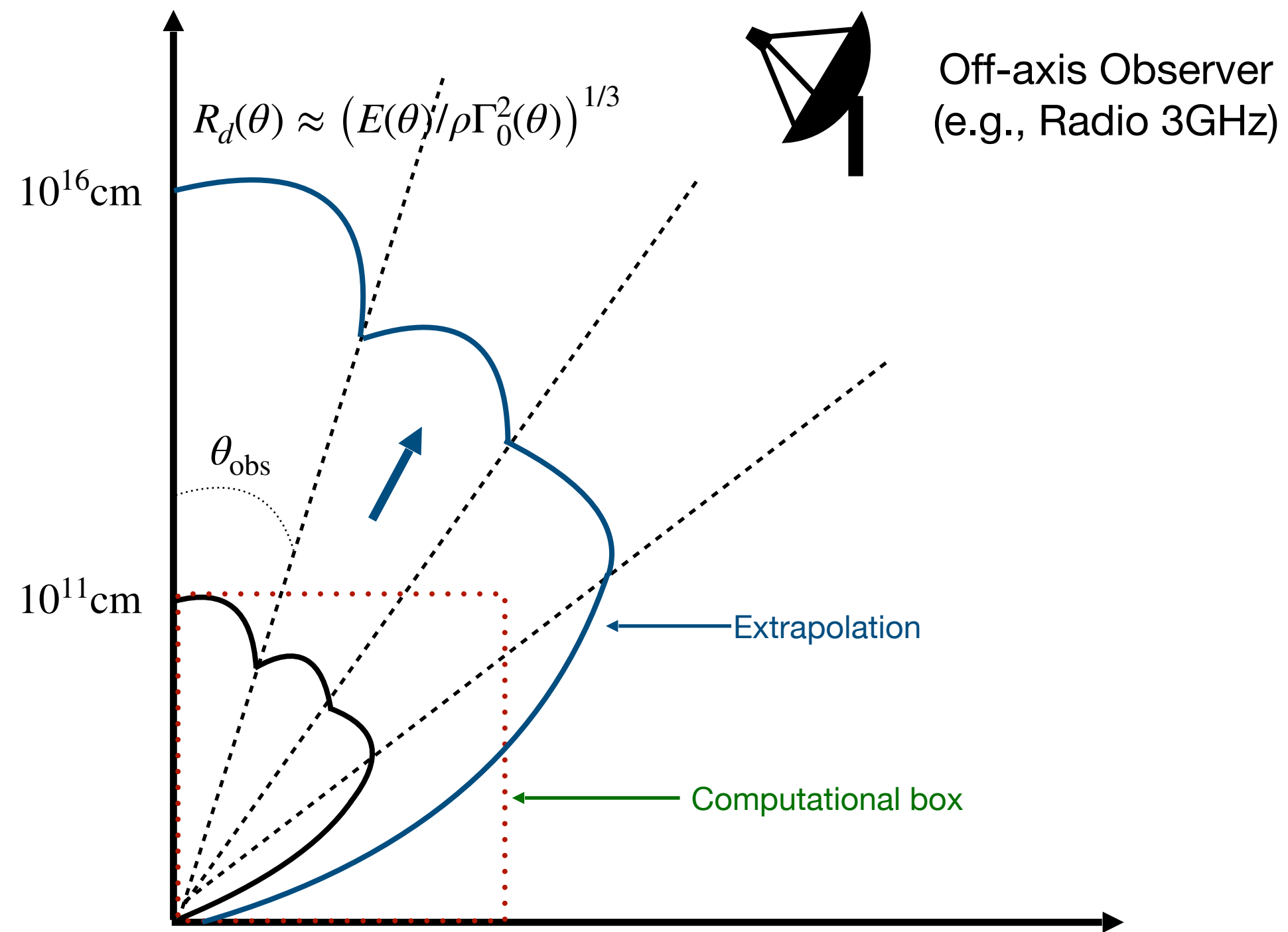
Yesterday, Talk by Emma Dreas: The kinetic component dominate at scales $> 10^{11}$ cm



We follow the standard afterglow estimation
(Sari, Piran & Narayan 1990; Granot & Sari 2002)

- Blandford & Mckee 1976 model
- Synchrotron emission. Magnetic field amplified in the shock front.

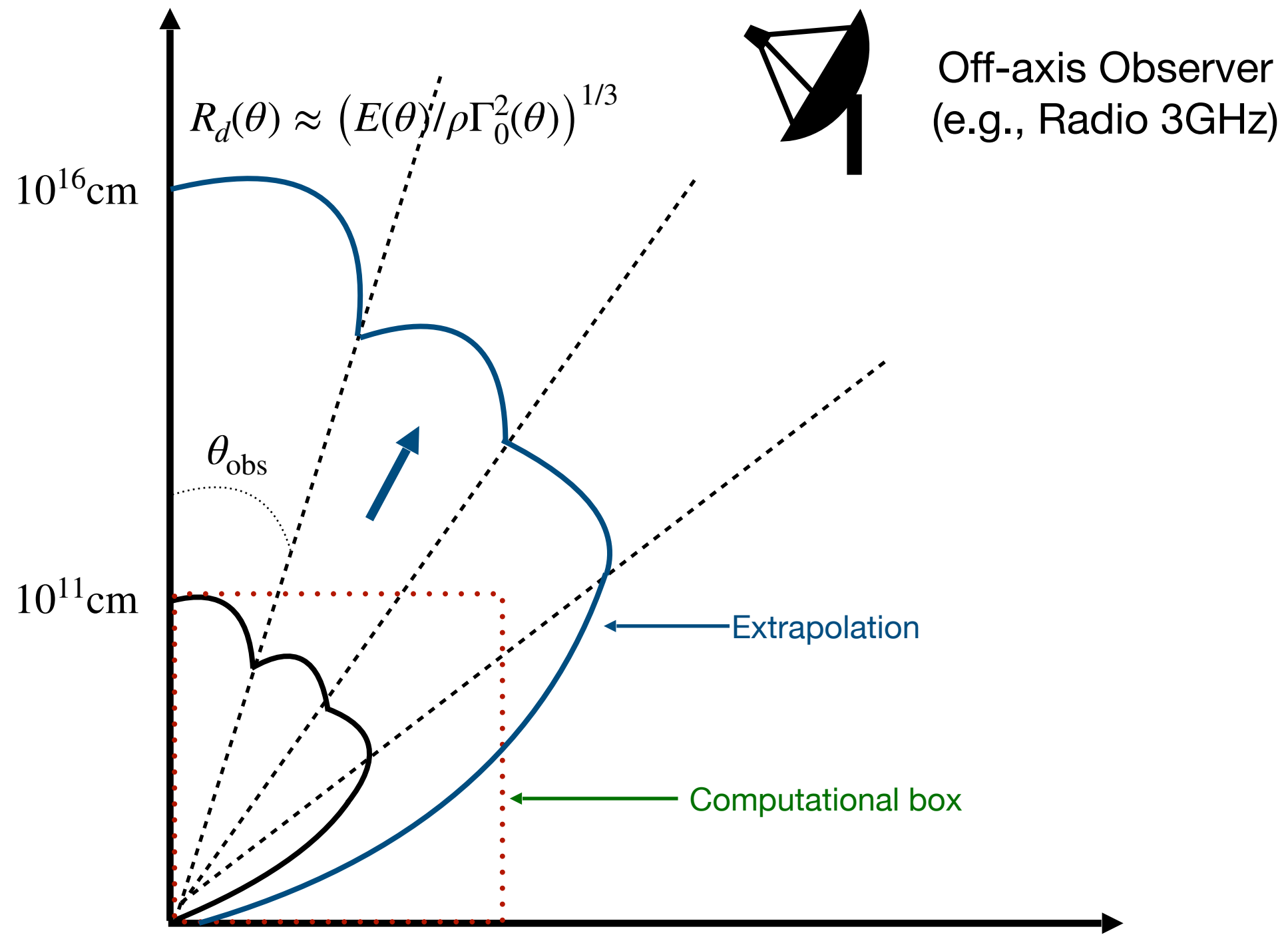
Yesterday, Talk by Emma Dreas: The kinetic component dominate at scales $> 10^{11}$ cm



We follow the standard afterglow estimation
 (Sari, Piran & Narayan 1990; Granot & Sari 2002)

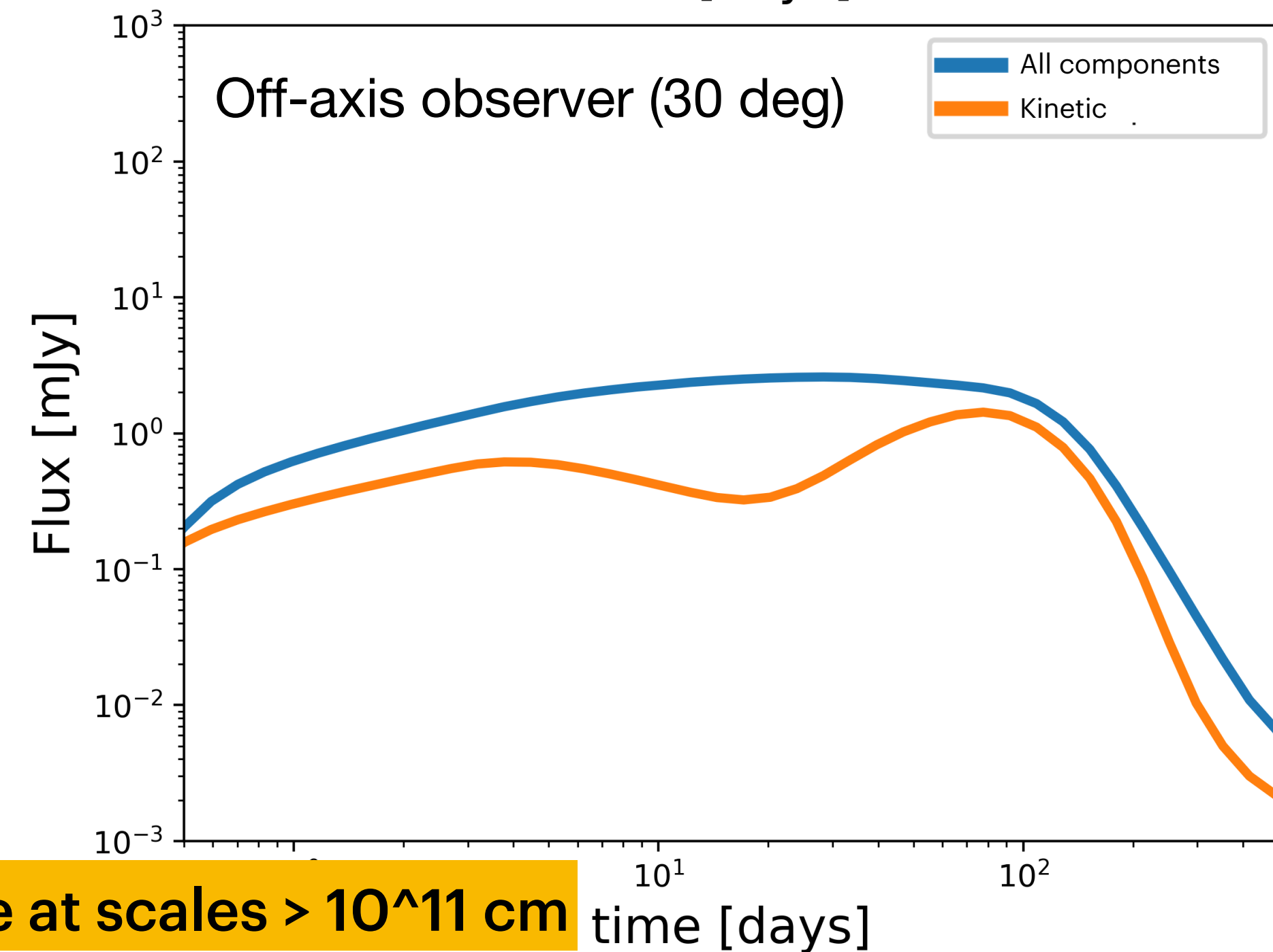
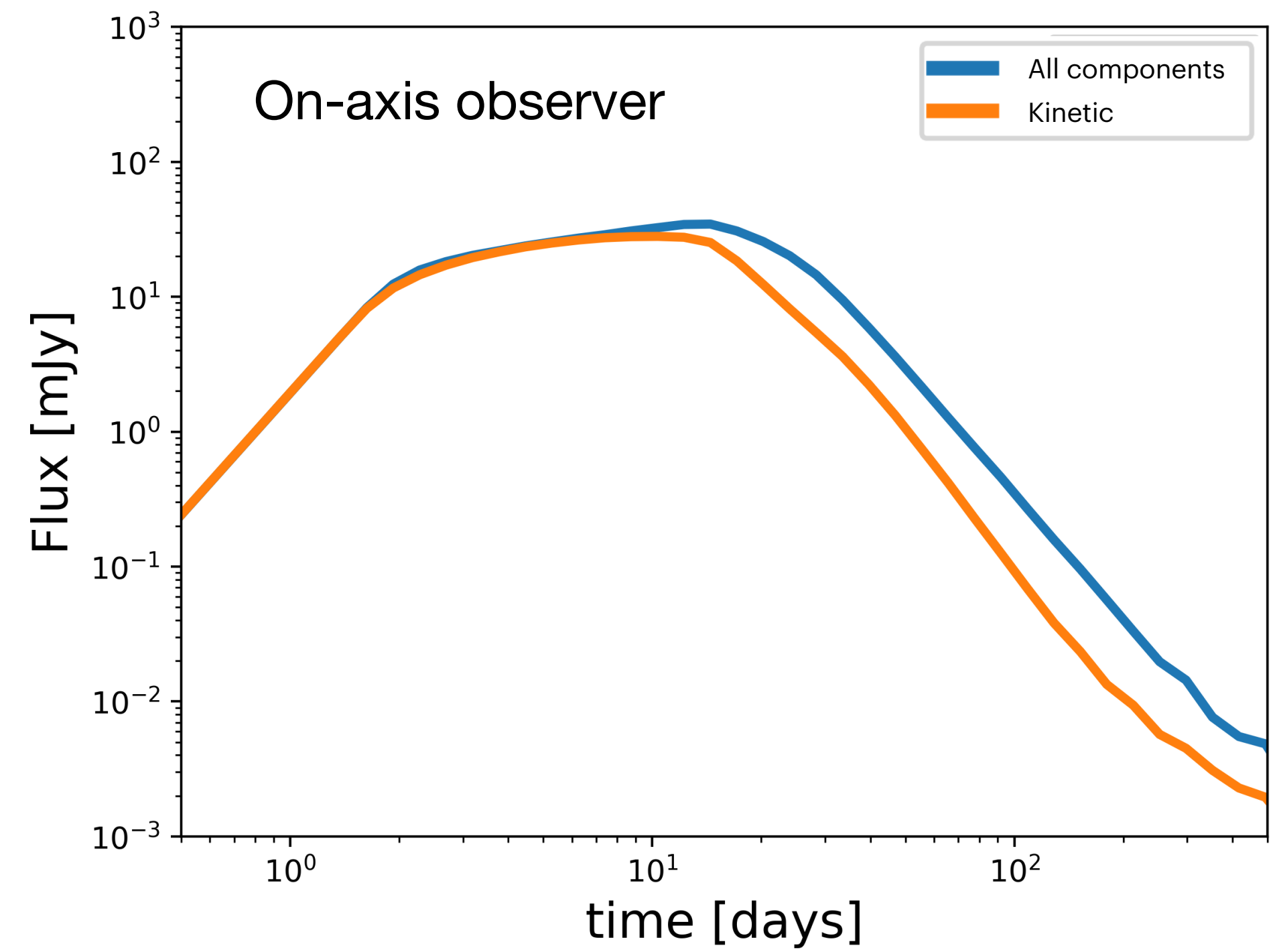
- Blandford & Mckee 1976 model
- Synchrotron emission. Magnetic field amplified in the shock front.

Yesterday, Talk by Emma Dreas: The kinetic component dominate at scales $> 10^{11}$ cm



We follow the standard afterglow estimation
(Sari, Piran & Narayan 1990; Granot & Sari 2002)

- Blandford & Mckee 1976 model
- Synchrotron emission. Magnetic field amplified in the shock front.



Yesterday, Talk by Emma Dreas: The kinetic component dominate at scales $> 10^{11}\text{ cm}$

Conclusions

- At scales $r \sim 10^8 \text{cm}$ and $t \sim 2\text{s}$, the jet is still magnetized. In this scenario, strong shock conditions imposed far from the black hole could be not consistent with the central engine activity.
- At intermediate scales, the kinetic energy is still not dominant, therefore, an analytical expansion for estimates of afterglow radiation could not represent a correct interpretation.
- Failed jets are produced in a low-magnetized scenario. It happens when the BZ mechanism is not activated. It is more related to the previous evolution of the progenitor star (special configuration of the magnetic field) and not to the dynamics of the jet.

